THE UNIVERSITY OF MANITOBA

LOCALIZED SPIN FLUCTUATIONS IN RUTHENIUM BASED ALLOYS

by

Francis Chun-Chung KAO

A THESIS

SUBMITTED TO THE FACULTY OF GRADUATE STUDIES

IN THE PARTIAL FULFILLMENT OF THE REQUIREMENTS OF THE DEGREE

OF MASTER OF SCIENCE

DEPARTMENT OF PHYSICS

WINNIPEG MANITOBA

OCTOBER 1973

ABSTRACT

Electrical resistivity measurements on several dilute Ru Cr and Ru Fe alloys have been made between the temperatures of 1.45° and 300° K.

The incremental resistivity for the Ru Cr alloys is temperature independent at low temperature. Above 75° K, deviations from Matthiessen's rule occur, and these are fitted on the basis of a 'Two Current Model.' For the Ru Fe system, the incremental resistivity is found to be temperature dependent, increasing as T^2 below about 170° K, but more slowly at higher temperatures. This temperature dependence is attributed to the scattering of conduction electron from the localized spin fluctuations: confirmatory evidence for this assignment comes from the analysis of existing measurements on the depression of the superconductivity transition temperature of Ru by the presence of Fe impurities.

Acknowledgement

I should like to express my gratitude to Professor Gwyn Williams under whose supervision this study was conducted. He not only suggested the general topic area but also contributed much to the analytical development of this study. In addition, his encouragement throughout my master's program is greatly appreciated.

I am also indebted to Professor P. Gaunt for his helpful discussions and suggestions.

Help has been given by Mr. M.E. Colp, and Mr. G. Roy.

Thanks are also due to Miss Selina Wan for the excellent job she has done in typing the manuscript.

TABLE OF CONTENTS

Chapter One

Introduction

Historical sketch

An electric field produces a drift of free electrons in metal and the resistance which this flow encounters is due to the scattering of electrons by obstacles in their paths. These are provided (a) by the thermal vibration of the crystal lattice, i.e. the phonons, and (b) by lattice imperfections such as impurity atoms, vacancies, and dislocations. Drude derived the dimensional formula for resistivity

$$\rho = \frac{m V_d}{n \ell e^2} \qquad (1.1)$$

in which n is the number, e is the charge and m is the mass of the electrons. Owning to the high "zero point" energy of the degenerated electron gas[1], the velocity V_d of the electron is essentially independent of temperature, thus reducing the problem to a calculation of the mean free path ℓ. Lorentz pointed out that electron-electron collision can be neglected so that ℓ is entirely determined by the condition of the lattice.

Bloch, making use of the fact that the mutual interaction between electrons can be disregarded, analyzed quantum mechanically the scattering of electrons by lattice vibration (i.e. by phonons) in a perfect lattice. This approach differs from that of Sommerfeld, who considered electron-electron processes against the background of a uniform ionic field. Bloch's theory deals with the effect of the periodic field of the lattice on a single electron. He found that the relation between resistance and temperature is identical with the semi-empirical formula proposed a little latter by Grüneisen on the basis of experimental data for various metals[1].

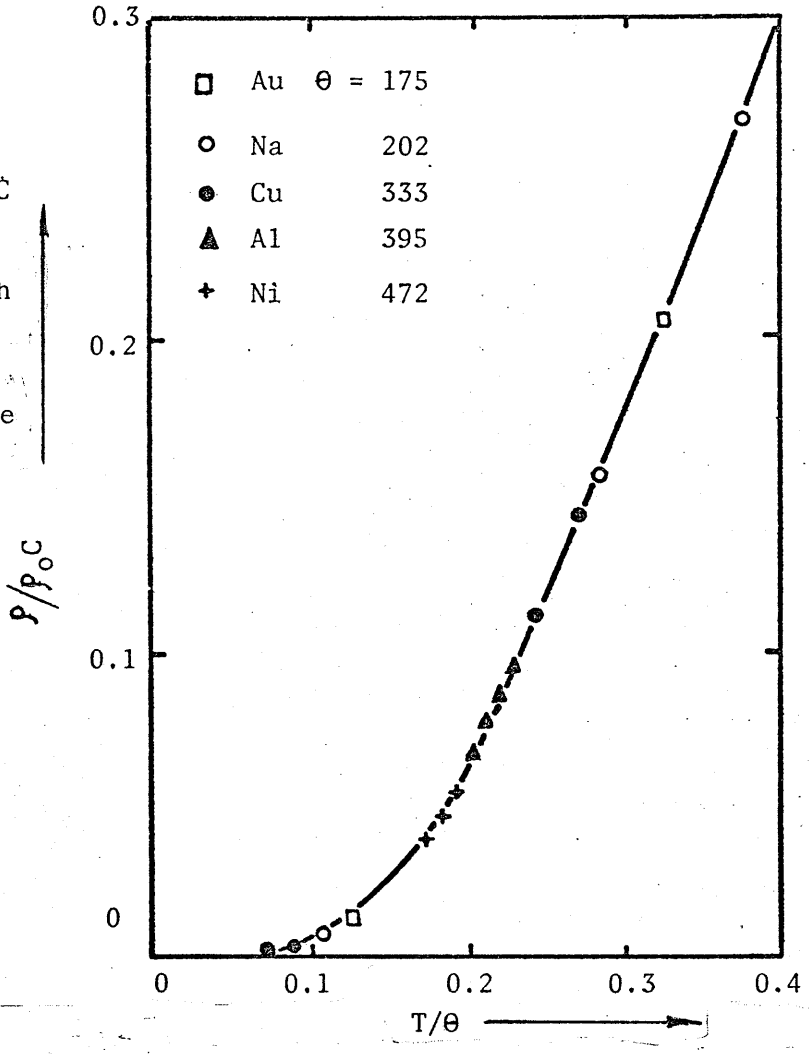

FIG. 1-1

The Reduced Resistivity $\rho/\rho_0 C$ For Five Metals Compared With Bloch-Grüneisen; Shown By The Full Curve.

[After Meissner]

$$\rho \propto \frac{T^5}{\theta_R 6} \int_0^{\theta_R/T} \frac{x^5}{(e^x - 1)\ (1 - e^{-x})}\, dx \qquad (1.2)$$

θ_R is the Bloch-Gruneisen characteristic temperature

This formula has much the same form as the Debye specific heat. This Bloch-Grüneisen formula works well as a first approximation, as is shown in Fig. (1-1), where the data for five different metals can be represented by a single curve. For high temperatures the integral in Eq. (1.2) approximates to $\frac{1}{4}\left(\frac{\theta_R}{T}\right)^4$ which leads to the classical result of $\rho \propto T$. Appreciable deviations due to the quantization of lattice vibrations only occur below $\sim 0.4\ \theta_R$ and at very low temperature T ($T \ll \theta_R$) the integral has a constant value, so that $\rho \propto T^5$. This region corresponds

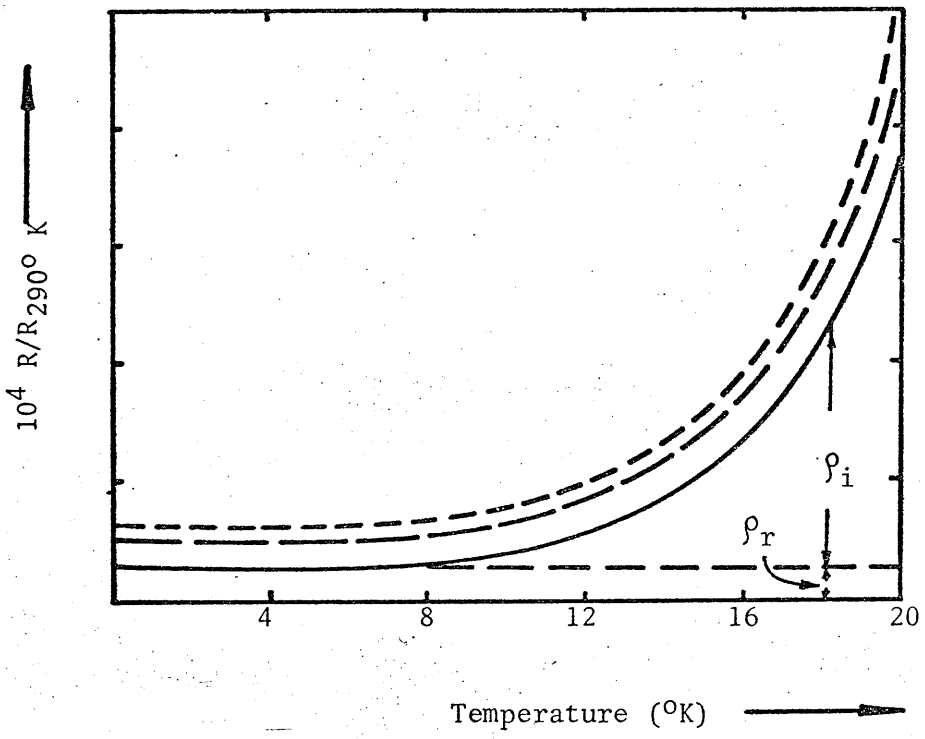

FIG. 1-2 Resistance Of Three Samples Of Sodium Of Different Purity. (MacDonald and Mendelessohn)

to the T^3 law for the lattice specific heat. At absolute zero, Bloch's theory leads to $\rho = 0$ for a perfect crystal.

The alkali metals can be expected to come closest to the quasi-free electron model used in Bloch's approximation and their resistivities were therefore made the subject of a careful study at Oxford[2].

A measurement of the resistivity on three sodium samples between the region of helium and hydrogen temperature was made and the results, shown in Fig. (1-2), yielded a power index of 4.85 which is in close agreement with the theoretical value of 4.89 derived from Eq. (1.2) for region between 8° K and 20° K. These experiments thus show that the Bloch T^5 law holds for the case of simple metals and that deviation from it must be due to departures from the quasi-free electron model. Such deviations have in fact been observed in all the other alkali metals as well as in those metals of other groups. The Bloch-Grüneisen formula suggests that the characteristic temperature θ_R should be constant, but in fact θ_R,

like Θ_D, in most cases is temperature dependent[3] and it has been found convenient to treat it, too, as a variable quantity, which is useful for the representation of resistivity data. Temperature dependence of Θ_R shows that there must be a departure from the simple quasi-free electron gas and this is confirmed when we examine the resistivities of multivalent metals. The work at Oxford has been extended to metals of the transition group and the investigated materials[2] (Pt, Pd, Rh, Ni, Co and Fe) all show the same type of deviation from the Bloch-Grüneisen function. At low enough temperature ($T < 6^{\circ}$ K) the power index becomes much smaller than 5, tending towards $\rho \propto T^2$. This behaviour may be due to electron-electron interaction which has been left out of our consideration.

So far only the effect of the thermal vibration has been taken into account and our considerations have referred to ideal metal crystals. While efforts have been made to approach such conditions experimentally, a certain amount of impurity as well as other crystal faults cannot be avoided. All these contribute to the resistance of the sample, but none of these imperfections vary appreciably with temperature and the limitation which they set to the mean free paths of electrons is therefore temperature independent. It has been postulated that the scattering introduced by lattice vibration and by imperfections should be independent of each other, and that resistivities caused by the two processes will be simply additive (Matthiessen's Rule). The over all resistance of a metal sample is therefore determined by the relative importance of the two scattering mechanisms. In ordered alloys, and pure metals, imperfection scattering is so small that except at very low temperature, they are completely masked by the scattering due to

lattice vibrations.

It can be seen from Fig. (1-2), that the curves for three specimens are strictly parallel which is a result of the Matthiessen's Rule.

$$\rho = \rho_i + \rho_r \qquad (1.3)$$

where ρ_i is the "ideal" resistivity due to scattering by lattice vibrations and ρ_r is the "residual" resistivity caused by the imperfections of the lattice.

Matthiessen's Rule seems to hold and this allows us to evaluate the "ideal" resistivity of the metal from data such as Fig. (1-2), for comparison with Bloch-Grüneisen function. In this aspect, any deviations from this simple pattern must appear disturbing.

Nordhiem (1931) studied the change of resistivity with change of concentration of impurity. When a very small concentration c of element A is introduced into the solvent element B, the electron may be considered as travelling through the perfect lattice of B, but occasionally they are scattered by the "aperiodic" potential around the A atoms, then we should expect the scattering probability to be proportional to the number of A atoms i.e. the concentration of A atoms. If c is not small, we cannot consider the alloy as consisting of perfect regions with the characteristics of B throughout which small point defects of A are interspersed.

There are a fraction c of A atoms and (1 - c) of B atoms in the system and the probability of an electron being scattered by either an A atom or a B atom will be proportional to c(1 - c). Thus the residual resistivity should be of the form

$$\rho_r \propto c(1 - c) \qquad (1.4)$$

which is known as the "Nordhiem's Rule", and will hold quite well in certain cases provided the two metals form a continuous range of solid solution and if no ordering or phase change occurs. One would also not expect it to be valid if the electron density or the Fermi surface changed with composition. Yet it does give an idea of the kind of behaviour which one might expect. Equation (1.4) suggests that a given concentration c of A in B should give the same resistivity increase as does the same concentration c of B in A. Mott (1934) has shown that this holds for metals which have similar atomic volume and electron configurations, e.g. Mg and Cd, Pd and Pt, Au and Ag.

Because of the complicated electronic states of the transition metals, alloy resistivities with transition elements as impurities will behave differently. The d-electrons of these transition metal impurities, since they are degenerate with the conduction band of the host, form virtual bound states on their own sites, thus the possibility of scattering of conduction electrons by these virtual bound states at the impurity sites arises and this invalidate the simple consideration of calculating the resistivity which we have discussed. Under this consideration, some alloys, in fact, show a resistance minimum and also sometimes a maximum at low temperature which make their behaviour more complicated.

These minima and maxima[4] in the resistivity have been observed below 10^{o} K in certain samples of gold, magnesium and other metals and seemed to be associated with traces of impurities. Much research has been

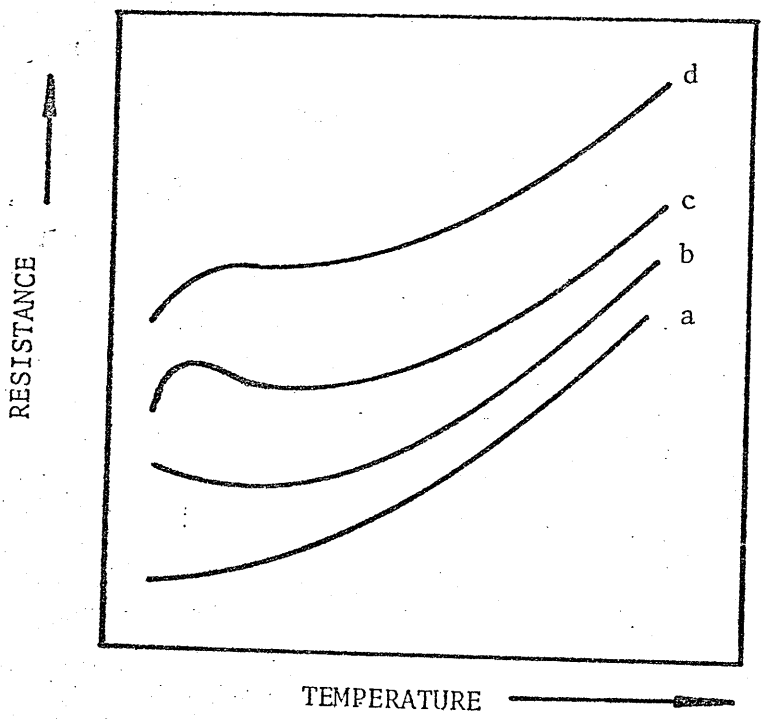

FIG. 1-3 Typical R-T Curves Of Alloys

(a) Non-Magnetic Case.

(b) With Magnetic Impurities (Resistance Minimun)

(c) Large Fraction Of Mag. Impurities.

(d) Still Larger Fraction.

G. J. Van Den Berg, in 'Progress in Low Temperature Physics'

devoted to this effect during the past ten years; at this point we briefly summarise the two theoretical models currently used to explain these phenomena, returning to a fuller discussion later.

J. Kondo[5] concluded that the resistivity minimum (curve b in Figure 1-3) is a direct consequence of conduction electrons scattering from a well defined spin (or magnetic moment) at the transition metal site. This minimum can be deduced from a simple model for the coupling between this magnetic moment and the surrounding conduction electrons —— the s-d exchange model —— as discussed by Zener[6], Kasuya[7], Yosida[8] and Frolich and Nabarro[9].

Calculations[5] based on the s-d exchange model, indicate that the resistivity of dilute magnetic alloys can be expressed by: -

$$\rho = aT^5 + c\rho_r - c\rho_1 \ln T \qquad (1.5)$$

where ρ_r is again the value of residual resistivity, a is constant, c is the concentration of magnetic impurity and

$$\rho_1 = -\rho_m \frac{3ZJ}{\epsilon_F} \qquad (1.6)$$

where J is the exchange integral between d-electron spin and the s-electron spin, E_F the Fermi energy, and

$$\rho_m = 3\pi mJ^2 S(S+1)\,(V/N) \Big/ 2e^2\hbar\,\epsilon_F \qquad (1.7)$$

For $J < 0$, this expression, Equation (1.5) would give a resistivity minimum at the temperature given by: -

$$T_{MIN} = \left[\frac{\rho_1}{5a}\right]^{1/5} c^{1/5} \qquad (1.8)$$

Kondo's calculation, based on the s-d model, assumes that the lifetime of the transition metal magnetic moment is infinite. This is only true when the Coulomb repulsion U between spin up and spin down electrons localised at the impurity site is infinite. When the restriction $U \longrightarrow \infty$ is relaxed, the magnetic moment at an impurity site aquires a finite lifetime, i.e. it fluctuates with time.

Kaiser and Doniach[10], using a two band approach, considered the effect of s electron scattering from d-level spin fluctuations localized within the impurity unit cell. On the assumption that the spin independent Coulomb potential associated with these isoelectronic impurities is vanishingly small, these authors predicted the following behaviour for the incremental resistivity, $\Delta\rho(T)$

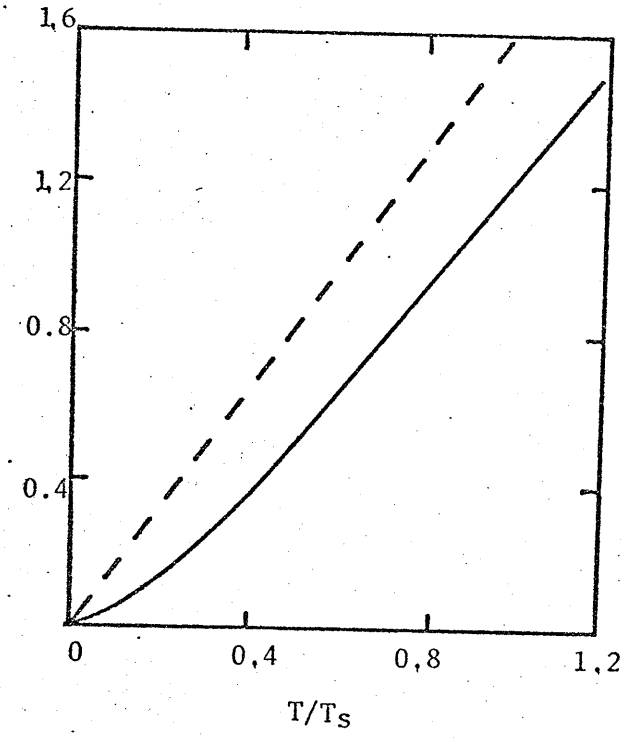

FIG-1-4

Universal curve for spin fluctuation resistivity calculation from Equation 1.33 the dotted line is the high temperature limit.

depending on temperature was predicted as following:-

$$\Delta\rho(T) \propto c\left(\frac{T}{T_{sf}}\right)^2 \quad \text{for } T \leqslant 1/4\ T_{sf} \quad \text{and}$$

$$\Delta\rho(T) \propto c\left(\frac{T}{T_{sf}}\right) \quad \text{for } T \geqslant 3/5\ T_{sf} \qquad (1.10)$$

where c is the impurity concentration and T_{sf} is termed the characteristic spin fluctuation temperature corresponding to the peak in the wave vector

averaged spectral density function A(w) for localized spin fluctuations (ℓsf). The behaviour predicted by Equation (1-10) is reproduced in Figure 1-4; and accounts qualitatively for the observed resistivity typically in ———————— transitional metal alloys like Rh Fe[11] and Ir Fe[12].

Having outlined the two basic theoretical approaches, we now proceed with a more detailed discussion of impurity states in alloys.

1.2 Screening

One of the simplest treatments of impurity atoms in a host metal is to consider the electrostatic field around the charged impurity as a perturbation in a solid. If we substitute an impurity ion for a host metal ion in the lattice, we put into the system a net charge which equals the difference in charge between impurity and host atoms. We can thus treat this impurity as if it were a simple point charge in a neutral background, and calculations can be made based on a free-electron gas model.

The perturbing potential can be written as:-

$$\delta U = \frac{Ze^2}{r} \exp\left[-\lambda r\right] \qquad (1.11)$$

where Z is the charge difference.

this potential behaves like that of the point charge near $r = 0$, for larger r this screened Coulomb potential falls off exponentially with distance, having a screening potential radius of $1/\lambda$. This short range potential is effective only close to the impurity site in a metallic

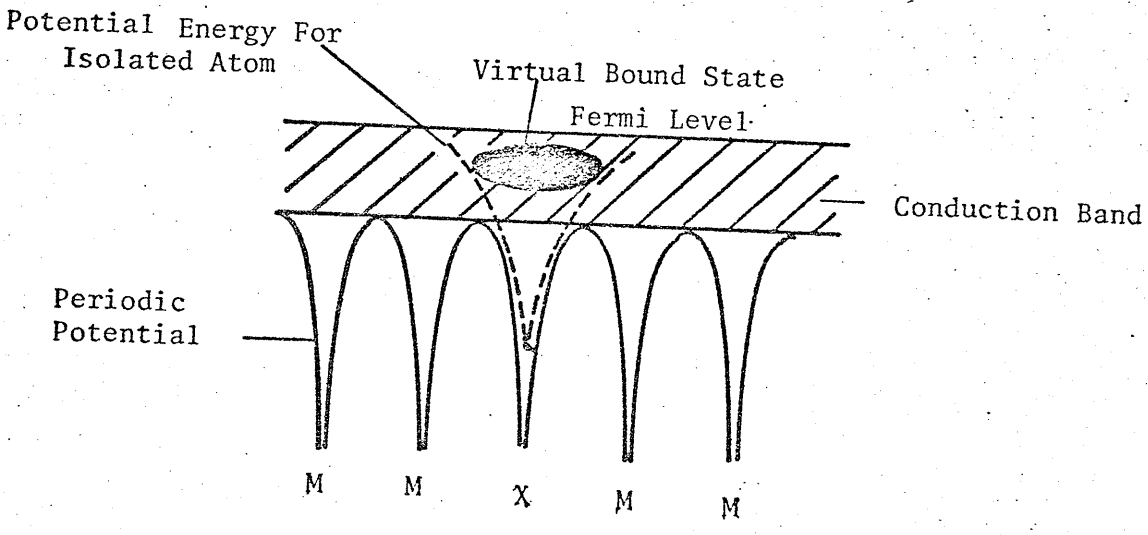

FIG. 1-5 Virtual d Level On X In MX.

enviornment (λ large) and is much longer ranged in a semi-conductor.

The impurity has introduced an excess nuclear charge which for electrical neutrality must be screened. The excess charge induced in the vicinity of the impurity can be obtained by integrating the change $\Delta\rho(r)$ (charge induced) in the density of states, and is given by[5]

$$4\pi\int_0^r \Delta\rho(r)\, r^2 dr = \frac{2}{\pi}\sum_\ell (2\ell+1)\left[\eta_\ell(\epsilon_F) - \frac{2k_F}{r}\sin\eta_\ell(\epsilon_F)\sin(2k_F r + \eta_\ell(\epsilon_F) - \ell\pi)\right] \tag{1.12}$$

where η_ℓ is the phase shift introduced in the ℓ th. partial wave by potential (charge) scattering.

For sufficiently large r , the second term may be neglected and hence Equation (1.12) gives the Friedel's Sum rule[13].

$$Z = \frac{2}{\pi}\sum_\ell (2\ell+1)\,\eta_\ell(\epsilon_F) \tag{1.13}$$

where Z is the excess impurity charge.

On differentiating Equation (1.12) with respect to r and keeping only the leading term, we find the radial dependence of the extra charge is given by $e\Delta\rho(r)$ where

$$\Delta\rho(r) = \frac{1}{2\pi^2 r^3}\sum_\ell (2\ell+1)\sin\eta_\ell(\epsilon_F)\cos(2k_F r + \eta_\ell - \ell\pi) \tag{1.14}$$

$\Delta\rho(r)$ oscillates in sign and tends to zero only as $1/r^3$. Consequently the screening charge in the neighbourhood of the impurity is not simply heaped up, but $\Delta\rho(r)$ assumes positive and negative values.

Assuming that phase shift for a particular ℓ shows a resonance at

ϵ_f it follows that when $\epsilon_F \ll \epsilon_f$, $\eta_\ell(k_F)$ will be small and the disturbance of the Fermi sea will also be small. At $\epsilon_F \gg \epsilon_f$, the phase shift approaches π and so the number of states below E_F increases by nearly $2(2\ell + 1)$ (including spin) as a result of screening the impurity, but the distrubance at large r is again small. At $\epsilon_F \approx \epsilon_f$, $\eta_\ell(k_F)$ will be close the $\pi/2$ so the scattering cross section for this ℓ th partial wave will be close to its maximum value.

The physical interpretation of the situation discussed above is accomplished in terms of virtually bound states that are spatially localized in the vicinity of the impurity site and energetically localized near ϵ_f.

$$\Delta\rho(r) = \frac{\alpha}{2\pi^2 r^3} \cos(2k_F r + \varphi)$$

for $r \longrightarrow \infty$

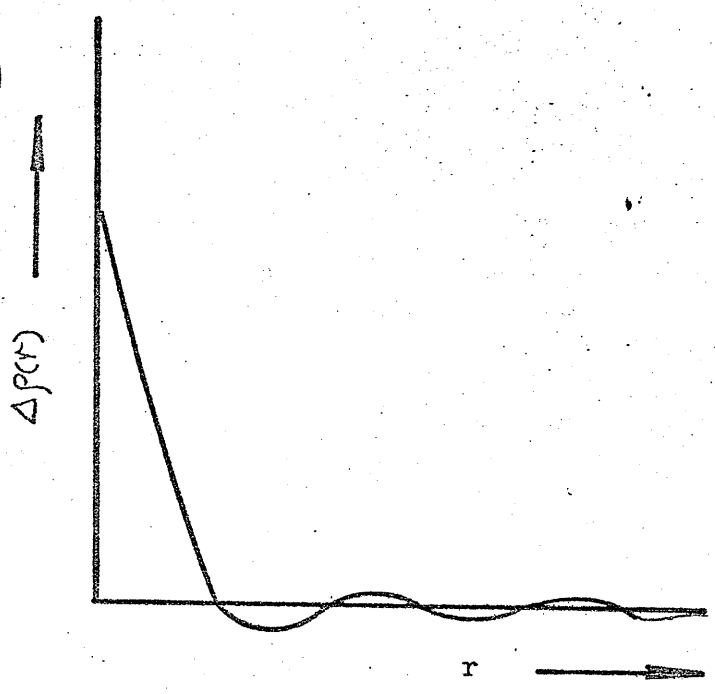

FIG.-1-6 Screening Of A Point Charge And Long Range Oscillation In Electronic Density.

1.3 Virtual bound states

For an isolated, single d electron atom, the d electron is bound for all time to the atomic core by the Coulomb force. This defines a true bound state. When such an atom is placed in metallic environment where the electron band widths are broad, the energy levels of this d electron would in general lie within the conduction band. As a result, this d electron decays rapidly into the continuum of one electron band states. The unbalanced excess charge then left at the impurity site is in fact screened out by the charge density $\Delta\rho$ built up around it (discussed previously). No particular electron forms this screening charge cloud

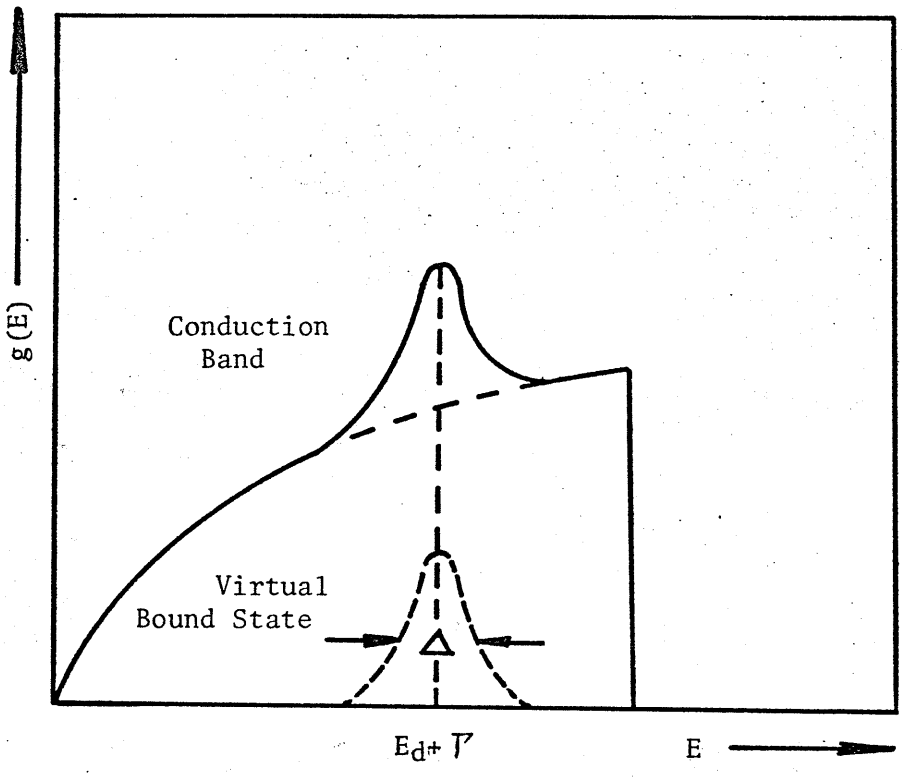

FIG.-1-7 Effect Of A Virtual Bound State On The Density Of States vs. Energy

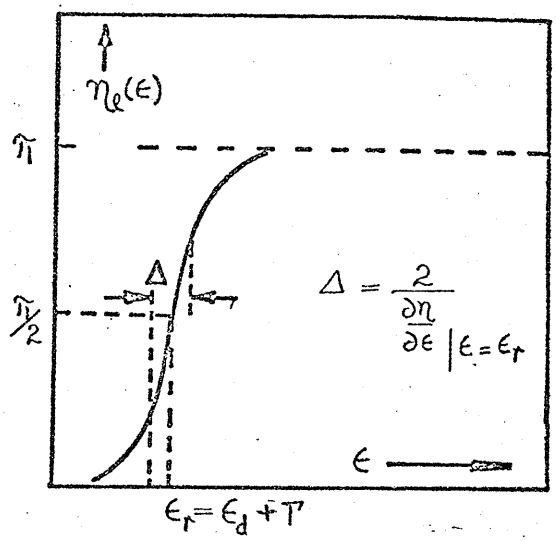

FIG. 1-8 Phase Shift For A Virtual & Bound State Of Width

permanently, but rather, in the time average sense, a net fixed amount of charge is accumulated. This is the 'Virtual Bound State'. The corresponding impurity states are not truely localized, but have a finite energy width Δ given by: -

$$\Delta = \frac{\pi\, N_0(E)}{F'(E)}$$

$$\text{with } F'(E) = P.P. \int \frac{N_m(\epsilon)\, d\epsilon}{E - \epsilon} \qquad (1.15)$$

$N_m(\epsilon)$ is the density of states in band m.

The tendency towards magnetism arises in a natural way from the electron-electron exchange potential. In a self consistant way within the frame work of the Hartree Fock theory[14], if this virtual bound level is sufficiently close enough to the Fermi level, the impurity atom might develop an exchange potential that polarizes the electrons in its vicinity, and thus produce a moment. In this limit the virtual bound d state energy can be written[15] as

$$E = E_d + \Gamma + i\Delta \qquad (1.16)$$

where E_d is the original d-state energy now shifted by an amount T (which is proportional to the mixing probability between s and d state) and broadened into a Lorentzian with an energy width Δ, given by Equation 1.15.

Further: -

$$\Gamma = P.P. \int \frac{|\langle d | H_{sd} | k \rangle|^2}{(E - E_k)} d^3k \qquad (1.17)$$

where $|d\rangle$ and $|k\rangle$ are the eigen functions of the impurity and conduction electron states respectively, and the density of states associated with this Lorentzian virtual bound state is: -

$$\rho_d(E) = \frac{(2\ell + 1)}{\pi} \frac{\Delta}{(\epsilon - E)^2 + \Delta^2} \qquad (1.18)$$

where $(2\ell + 1)$ arises from the orbital degeneracy in the absence of crystal field effects.

There is no doubt that the concept of virtual bound state is physically meaningful in the theory of electronic structure of dilute alloys involving transition elements and several properties of alloys of transition metals can be explained with this concept.

1.4 Localized magnetic moments

A localized magnetic moment occurs when the occupation of up spin virtual states is not equivalent to that for down spin. Figure-1-9. As an operational definition, a moment exists experimentally if the impurity contribution $\Delta\chi$ to the susceptibility is strongly temperature dependent in the form of a Curie law $\Delta\chi = C/T$ where C is the Curie constant $= \frac{N \mu^2}{3k_B}$, while temperature independent behaviour is taken to signify no localized magnetic moment, Sarachik et al[11] showed the existance of an one-to-one correspondence between the existence of strongly temperature dependent susceptibility and the appearance of a minimum

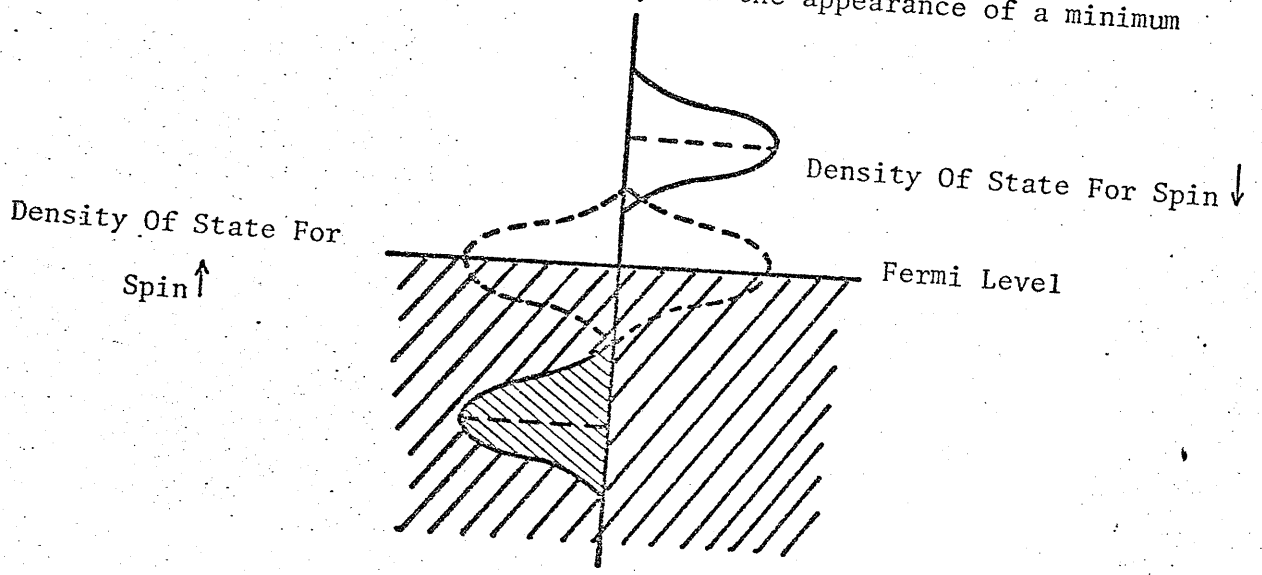

FIG.-1-9 Localized Magnetic Moment Arises From A Virtual Bound State

in resistance verses temperature plot.

The weak concentration dependence of the temperature of the resistance minimum ($\propto C^{1/5}$ Equation (1.8)) and the scaling of the low temperature resistivity with impurity concentration indicates that this effect does not arise from impurity — impurity interactions,

but is an isolated impurity effect.

The basic interaction responsible for such moment formation in a metal has been postulated to be the local particle-particle Coulomb interaction U between electrons of opposite spin at the impurity site. A large Coulomb interaction will tend to keep one and only one electron on the impurity site (in a one-orbital model). However, the up spin and down spin electrons at the impurity site and in the surrounding electron gas could be correlated via the local coulomb interaction, such that when a up spin (down spin) electron is on the site, a down spin (up spin) electron is nearby in the electron gas.

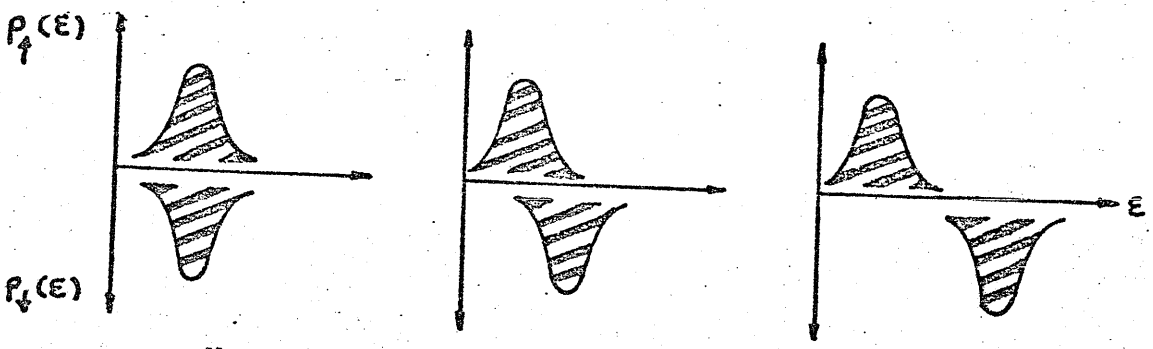

(a) $\frac{U}{\Delta} \ll 1$ (b) $\frac{U}{\Delta} \approx 1$ (c) $\frac{U}{\Delta} \gg 1$

FIG.-1-10 Non-Magnetic Magnetic

In figure 1-10 we show the density of states for spin up, $\rho_\uparrow(\epsilon)$, and spin down, $\rho_\downarrow(\epsilon)$, as a function of U/Δ. Figure 1-10(a) for which $U/\Delta \ll 1$ means that the number of spin up and spin down electrons is always equal, and hence the impurity state is non magnetic. Figure 1-10(b) depicts the situation fpr which spin fluctuations are important, while Figure 1-10(c) approaches the s-d model regime.

Wolff has considered the scattering of Bloch waves from a single substitutional impurity atom in an otherwise perfect crystal.

Under the assumption that the wave function may be expanded in terms of Wannier functions from a single band—— that is neglecting interband matrix elements of the impurity Potential V

FIG.-1-11

Typical Plot Of $F_m(E)$ vs. E

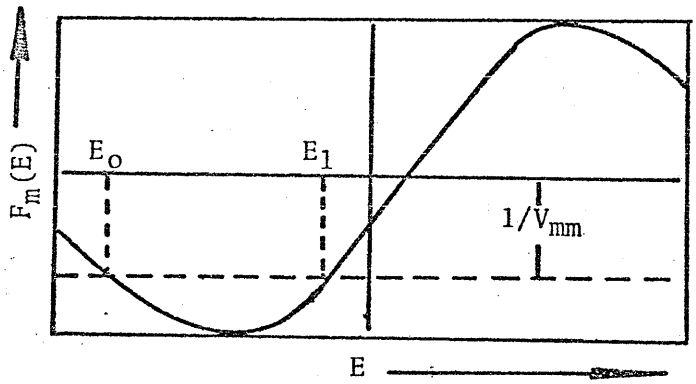

$$F_m(E) = P.P.\int \frac{P_m(\epsilon)\, d\epsilon}{(E - \epsilon)}$$

$$\left\langle a_n(\vec{r} - \vec{R}_i) \middle| V \middle| a_{n'}(\vec{r} - \vec{R}_j) \right\rangle = V_{nn'}\, \delta_{nn'}\, \delta(\vec{R}_i - \vec{R}_o)\, \delta(\vec{R}_j - \vec{R}_o) \tag{1.19}$$

where a_n and $a_{n'}$ are the Wannier's funductions of conduction electron states at R_i and R_j respectively.

where R_o is the location of the impurity. With this approximation and using the method of Koster and Slater[16], the scattering wave function will be given by: -

$$\Psi = \sum \vec{R}_i \left[U_m(\vec{R}_i) a_m(\vec{r} - \vec{R}_i) \right] \tag{1.20}$$

where

$$U_m(\vec{R}_o) = \frac{e^{i\vec{k}\cdot\vec{R}_o}}{\left\{ \left[1 - V_{mm} F_m(E) \right] + i\pi V_{mm} N_m(E) \right\}} \tag{1.21}$$

with $F_m(E)$ and $N_m(E)$ as defined in Equation (1.15)

We wish to consider the factor $\left[1 - V_{mm} F_m(E)\right]$ that appears

in the denominator of Equation (1.21). In particular, we are interested in the zeros of this expression, which gives the maximum value of $U_n(R_o)$.

The zeros of this expression $\left[1 - V_{mm}\ F_m(E)\right]$ are then determined by the intersections of the line $1/V_{mm}$ with $F_m(E)$ as in Figure (1.10). For an attractive potential, there are two roots (labeled E_o and E_1). It is clear from the diagram that the roots occur in pairs, and that for the simple sort of $F_m(E)$ curve that we are considering, there can either be zero or two of them. We are now interested in the case in which there are two roots and will particularly focus our attention on that root of the expression at which $F_m(E)$ has a negative derivative. (at $E = E_o$ in Figure (1.11)).

Now consider the effect of addition of a spin dependent potential to V_{mm}, dropping the band subscript, the two potentials for spin up and

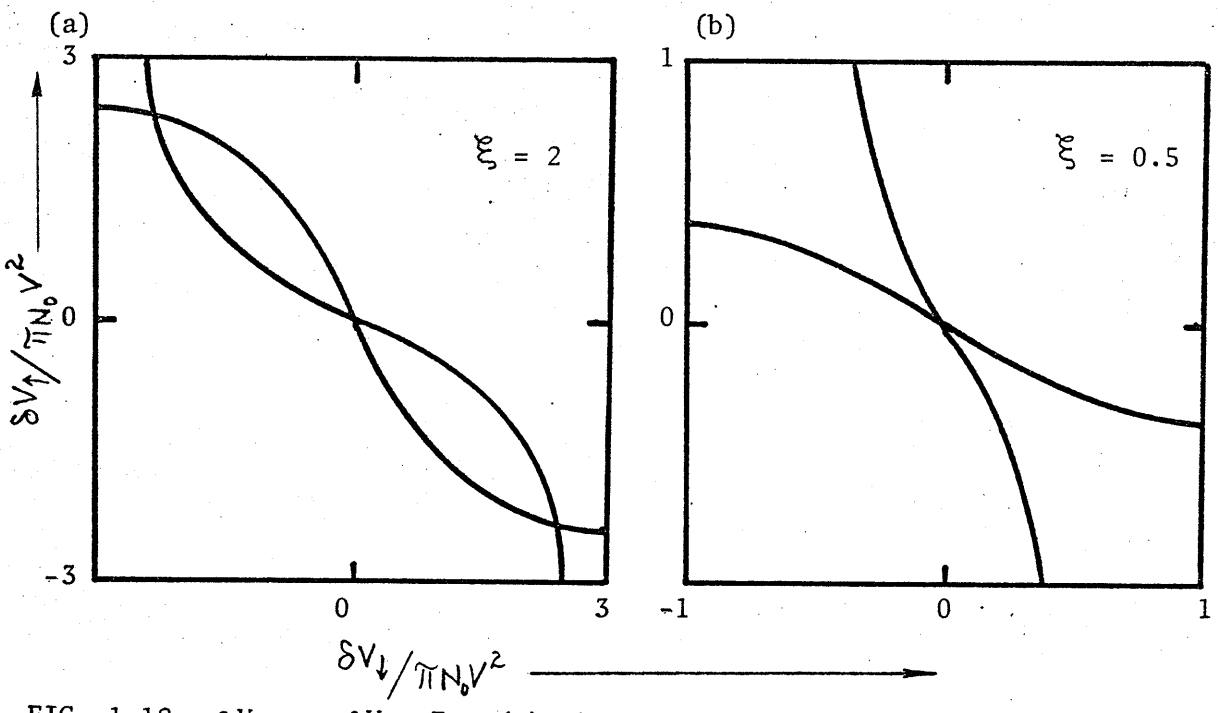

FIG.-1-12 $\delta V_\uparrow$ vs. $\delta V_\downarrow$ For (a) The Virtual Level Is At The Fermi Level And Polarized (b) Unpolarized

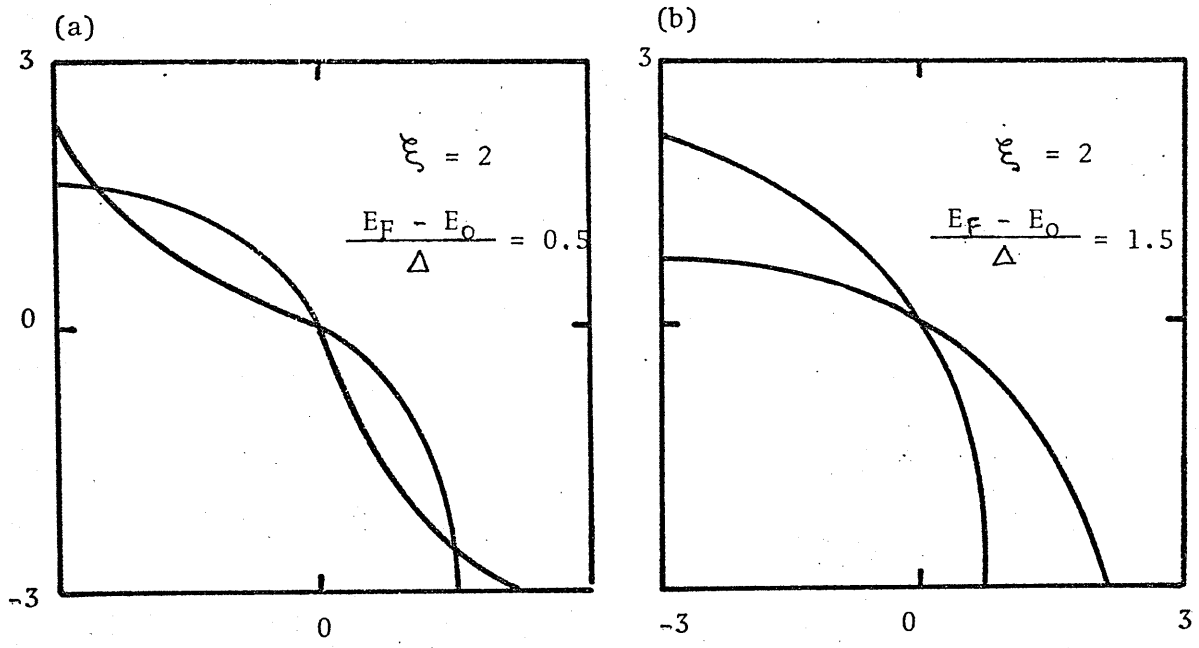

FIG.-1-13 $\delta V_\uparrow$ vs. $\delta V_\downarrow$ (a) For A Case In Which The Virtual Level Is Slightly Displaced From Fermi Level, But Remain Polarized. (b) Shifted Far Enough From The Fermi Level To Destroy Polarization.

spin down electrons are $V + \delta V_\uparrow$ and $V + \delta V_\downarrow$, then Equation (1.18) will become

$$U_\uparrow(\vec{R}_o) = \frac{e^{i\vec{k}\cdot\vec{R}_o}}{\{[1 - (V + \delta V_\uparrow) F(E)] - i\pi (V + \delta V_\uparrow) N(E)\}} \qquad (1.22)$$

and a similar expression holds for $U_\downarrow(\vec{R}_o)$. Wolff calculated the change in the Hartree Fock field of impurity, and under the self consistent limitation which requires that the change in the two matrix elements of V_{HF} be equal to $\delta V_\uparrow$ and $\delta V_\downarrow$.

$$\delta V_\uparrow = \frac{J}{\pi (V + \delta V_\downarrow)^2 F'} \left\{ \tan^{-1}\left[\frac{(E_F - E_o)F'}{\pi N_o} + \frac{\delta V_\downarrow}{V \pi N_o (V + \delta V_\downarrow)}\right] + \frac{\pi}{2} \right\}$$
$$- \frac{J}{\pi V^2 F'} \left\{ \tan^{-1}\left[\frac{F'(E_F - E_o)}{\pi N_o}\right] + \frac{\pi}{2} \right\} \qquad (1.23)$$

where $J = \iint |\alpha(r - R_o)|^2 \, |\alpha(r' - R_o)|^2 \frac{e^2}{|\bar{r} - \bar{r}'|} d^3r \; d^3r'$

the exchange intergal. With the limit $\frac{\delta V_\downarrow}{V} \ll 1$ and $E_o = E_F$

$$\delta V_\uparrow = \frac{J}{V^2 F'} \cdot \tan^{-1}\left[\frac{\delta V_\downarrow}{\pi N_o V^2}\right]$$

$$\delta V_\downarrow = \frac{J}{V^2 F'} \cdot \tan^{-1}\left[\frac{\delta V}{\pi N_o V^2}\right] \qquad (1.24)$$

Typical plots of these equations are illustrated in Figure (1.12A) and Figure (1.12B) with $J/\{\pi^2 V^4 P_o F'(E)\} > 1$ and < 1 respectively. There are three roots; one with $\delta V_\uparrow = \delta V_\downarrow = 0$ which implies no localized moment, and two stable ones with $\delta V_\uparrow = -\delta V_\downarrow = \pm$ (constant).

When considering the situation with $E_0 \neq E_F$, it follows from the graphs in Figures (1.13a) and (1.13b), that a stable moment exists if

$$\frac{\partial (\delta V_\uparrow)}{\partial (\delta V_\downarrow)} > 1 \quad \text{or}$$

$$\left| \frac{J}{\pi^2 V^4 \quad F'(E)} \right| > \frac{(E_f - E_o)^2 + \Delta^2}{\Delta^2} \qquad (1.25)$$

i.e. a relatively sharp level close to the Fermi surface favours the formation of a moment.

Friedel emphasized that the virtual bound state corresponds to a maximum in scattering cross-section. If the virtual level occurs at the Fermi level, it should give rise to an unusually large residual resistance. This, according to the Anderson and the Wolff models, is

just the situation in those alloys in which the Fe atoms first begin to acquire a moment.

1.5 The s-d Exchange Model.

The s-d exchange model was first proposed by Zener[6] and Frohlich and Nabarro[9], they considered the exchange interaction between d-electrons, localized at the impurity sites, and s-electrons itenerant over the range of the crystal. The Exchange Hamiltonian can be written as:-

$$H_{sd} = -2J\,\underline{s}\cdot\underline{\sigma} \qquad (1\text{-}26)$$

where J is the exchange integral defined in the previous section, $\underline{s}$ and $\underline{\sigma}$ are spin operators for d-electron and the conduction electron respectively.

Working with the First Born Approximation[4], one finds that the transition probability, by the Golden Rule, is given by:

$$J^2 < M^2 > N(E) = 1/3\, J^2\, S(S+1)\, N(E) \qquad (1\text{-}27)$$

which shows no temperature dependence.

Kondo[4] calculated up to the Second Born Approximation the scattering of conduction electron by the s-d interaction, and found that the resistivity is given by:

$$\rho(T) = K J^2 S(S+1) \left[1 + 4JN(0) \ln\frac{k_B T}{D} \right] \qquad (1\text{-}28)$$

where K is the constant and D is the half width of the d-band.

The second term diverges logarithmically at the temperature $T \lesssim T_K$ where T_K is the Kondo temperature given by:

$$T_K k_B = D \exp\left[-1/|J|\, N(0) \right] \qquad (1\text{-}29)$$

The origin of this divergence lies in Pauli principle restriction on the intermediate states, which comes into play as a result of non-commutativity of the spin operators. As a matter of fact, the resistivity

minimum is indeed a result of such a many body effect.

This logarithmic singularity of Equation (1-28) will be suppressed by an applied external magnetic field or by many other factors[5]. This applied magnetic field disturbs the free motion of the spin and prevents its internal degree of freedom from being fully effective in causing the singularity. A similar effect is also expected for the spin in a super-conductor where a finite energy is needed to excite a pair of quasiparticles.

Since Kondo's discovery of a logarithmic divergence in perturbation theory for the scattering of conduction electrons from magnetic impurities in metals, a large amount of experimental and theoretical work has been devoted to this problem. Recently Heeger[17] suggested that Kondo effect can be interpreted as arising from an indirect-electron-electron interaction via the magnetic impurity. From this point of view, he speculated that the spin lattice relaxation of this localized spin should destroy this effective interaction, and showed experimentally in a recent letter[18] that it was indeed the case that the anomalous term in the resistivity fitted the following relation:

$$\frac{\rho(T)}{c} = A + B \ln (T^2 + \theta^2)^{\frac{1}{2}} \qquad (1\text{-}30)$$

where A and B are constants and O is identified with T_{sf} the sf temperature, previously mentioned and is both impurity concentration and temperature dependence. The sign of the constant B has been studied[19,20] and found to depend on the screening charge calculated by Friedel Sum rule in the following manner:

$$B \propto \cos (1/5\ \eta Z) \qquad (1\text{-}31)$$

which shows that for $Z < 5/2$ or $Z > 15/2$, B is positive, which implies that the incremental resistivity $\Delta\rho(T)$ will be increasing as the temperature increases, and decreases when B is negative, i.e. $5/2 < Z < 15/2$.

1.6 Localized spin fluctuation.

Based on extensive experimental and theoretical effort, considerable progress has recently been made in formulating a reasonably consistent description of localized impurity states associated with first row transitional impurities in noble metals[5,17]. In dilute limit, the incremental resistivity $\Delta \rho(T)$ due to the presence of these impurities is found to increase anomalously with decreasing temperature, and at temperature well below T_K the Kondo temperature, $\Delta \rho(T)$ increases far less rapidly than one predicts in Equation (1-30) and typically having the form as[20]:

$$\Delta \rho(T \longrightarrow 0) = \Delta \rho(0) \left[1 - \left(\frac{T}{T_K}\right)^2 \right] \qquad (1\text{-}32)$$

Calculation based on this H_{sd} Hamiltonian do not reporduce the limiting temperature dependence [21,22] given in Equation (1-32). However, a unified description of these electrical proporties of such alloys has recently been achieved via the localized spin fluctuation (ℓ ,s,f) model[10]. Lederer and Mills[23] were the first to use a model of this type to calculate the scattering of s-conduction electrons from time dependent fluctuation of the magnetization at the site of a nearly magnetic transition metal impurity. If the ℓ .s.f. are slow enough equilibriate in an applied magnetic field or to flip the spin of a condition), its temporary magnetic moment may have sufficient time to equilibrate in an applied magnetic field or to flip the spin of a conduction electron, and so will contribute a Curie susceptibility and a logarithmic resistivity —— an impurity in the slow ℓ .s.f. regime[24] therefore appears to be (weakly) magnetic[25].

In an extention of the Lederer-Mills model, Kaiser and Doniach showed for isoelectronic alloys that the resistivity due to localized spin fluctuation scattering in general can be represented by this dimensionless expression.

$$\tilde{\rho} = \frac{1}{\tilde{T}} \int \frac{d\tilde{w}\ \tilde{w}^2}{\left[\exp\left(\frac{\tilde{w}}{\tilde{T}}\right) - 1\right]\left[1 - \exp\left(-\frac{\tilde{w}}{\tilde{T}}\right)\right]\left[1 + \tilde{w}^2\right]} \tag{1.33}$$

where $\tilde{T} = \frac{T}{T_{sf}}$, and $\tilde{w} = \frac{w}{k_B T_{sf}}$

T_{sf} is the spin fluctuation temperature defined[18] as:

$$T_{sf} = \frac{\left[1 - UN_i(E_F)\right]}{k\,\pi\,N_i(E_F)} \tag{1.34}$$

where U is the Coulomb repulsion between localized d-electrons in the Anderson model and $N_i(E_F)$ is the density of states at Fermi level.

In low temperature limits, one can obtain an analytic expression for $\tilde{\rho}$. As temperature $\longrightarrow 0$, the term $\tilde{w}^2$ in the demoninator of Equation (1.33) can be neglected and hence

$$\rho(T \longrightarrow 0) = \frac{\pi^2}{3} \left(\frac{T}{T_{sf}}\right)^2 \tag{1.35}$$

which is the low temperature behaviour found by Lederer and Mills[23]. As the temperature

$$\rho(T \longrightarrow \infty) = \frac{\pi}{2} \left(\frac{T}{T_{sf}}\right) \tag{1.36}$$

which shows that $\tilde{\rho}$ is linear in T in high temperature limit for any temperature-independent spectral density A(w) as illustrated by the similar behaviour of the localized spin fluctuation and phonon resistivity components.

The universal curve for spin fluctuation resistivity as calculated from Equation (1.33) and illustrated in Figure 1- 4 exhibits a transition from T^2 to T dependence at approximately 0.25 T_{sf}. When at higher temperature, the temperature dependent portion of the spectral density A(w) has to be taken into consideration, the Kaiser and Doniach model predicts a resistivity that flattens off rapidly, (refer to Figure 1- 4) a result which qualitatively is in agreement with experiment[26,11].

A strong exchange enhancement in the host metal will produce a spin fluctuation resistivity component for the pure metal. The T^2 resistivity component, such as for Pd[17] at low temperature is thought to arise largely from "spin fluctuation scattering[21]". Kaiser and Doniach assumed that Matthiessen's Rule holds and the resistivity components are additive, then:

$$\rho_{imp}(T) = \rho_{alloy}(T) - \rho_{host}(T) \qquad (1.37)$$

and $\rho_{imp}(T)$ can be separated into two components,

$$\rho_{imp}(T) = \rho_{mag}(T) + \rho_{non\text{-}mag.} \qquad (1.38)$$

where $\rho_{non\text{-}mag.}$ is of the temperature independent resistivity (equals to $\rho_{imp}(0)$) due to non-magnetic scattering from impurities.

Experimentally, the localized spin fluctuation resistivity in the host is less interesting than that of the impurity, since in the host, the T^2 law will typically extended to higher temperatures and cannot easily be separated from phonon resistivity.

When plotting the dimensionless ratio $\tilde{\rho}$ in Equations (1-35) and (1-36) against T^2 and T respectively, the slopes will be given:-

$$M_L \text{ (low temperature limit)} = \frac{\pi^2}{3} \cdot \frac{1}{T_{sf}^2} \quad \text{and}$$

$$M_H \text{ (high temperature limit)} = \frac{\pi}{2} \cdot \frac{1}{T_{sf}} \qquad (1.39)$$

and the spin fluctuation temperature T_{sf} will be given by the ratio of M_H to M_L.

$$T_{sf} = \frac{2\pi}{3} \cdot \frac{M_H}{M_L} \qquad (1.40)$$

1.7 Superconductivity

The existance of superconductivity in metals discovered by Kamerlingh Onner in 1911, is not a property of the individual atom, but due to the structure of the electronic energy spectrum of the metal or alloy. Frohlich attempted to explain that the superconductivity phenonimon is due to interactions involving the electrons, but through the intermediary of the lattice, i.e. via the electron-phonon interaction. Bardeen, Cooper and Schrieffer[27,28] (BCS), based on this idea, concluded that the normal states of metals or alloys are represented by the Bloch's model, while for the superconducting ones, the electron pairs (Cooper pairs) of opposite spin and momentum are invoked.

On the basis of the BCS theory the superconducting transition temperature T_C of the system is given by

$$T_C = 1.140_D \, e^{-1/g} \qquad (1.41)$$

where g measures the strength of this electron-phonon coupling.

Several calculations have been made of the depression of T_C on alloying. Recent calculations by Ratto and Blandin[29] and by Kaiser[30], which apply directly to the systems of interest here, yield:

Calculation[29,30] of T_c for non-magnetic alloys has the carried out, for large half width Δ ($\simeq$ 1.eV) and at low temperature $T \longrightarrow 0$, the ratio of the critical temperature (the superconducting transitional temperature) T_c of the alloy to that of the pure host is given by:

$$\frac{T_C}{T_{CO}} = \exp \frac{-\alpha^* + \beta^*}{\lambda (1 - \beta^* c)}$$

where α^* and β^* are constants defined by

$$\alpha^* = \frac{N_d(E_F)}{N(E_F)}$$

$$\beta^* = \frac{N_d(E_F)^2 U_{eff}}{(2\ell + 1)}$$

The number of impurity states.

$$N_d(E_F) = \frac{(2\ell + 1)}{\pi} \frac{\Delta}{\left[\Delta^2 + E_d^2\right]},$$

the Effective Coulomb Repulsion Potential

$$U_{eff} = \frac{U}{1 + \frac{U}{\pi E_d} \tan^{-1}\left(\frac{E_d}{\Delta}\right)} \qquad (1.42)$$

and λ is the characteristic coupling constant for the pure host.

The critical concentration c_t of impurity with which superconduction of the alloy is completely supressed will be given by:

$$c_t = \frac{1}{\beta^*} = \frac{(2\ell + 1)}{[N_d(E_F)]^2 U_{eff}} \qquad (1.43)$$

Reference

1. K. Mendelssohn, F.R.S. 'Cryophysics' Interscience Publishers Ltd., London, (1960).

2. P. G. Klemens, 'Solid State Phys.' 7, 1-99, (1958).

3. D. K. Mac-Donald, 'Properties of Metal at low temperature' Progr Metal Phys. 3, 55-75, (1952).

4. J. Kondo, 'Resistance Minimum in Dilute Magnetic Alloys.' Progr. of Theoretical Phys. Vol. 32, No. 1, July, (1964).

5. J. Kondo, 'Solid State Phys.' Vol. 23. Edited by Frederick Seitz, David Trunbull and Henry Ehrenreich, Academic Press, New York, (1969).

6. C. Zener, Phys. Rev. 87, 440, (1951).

7. T. Kasuya, Progr. Theor. Phys. 16, 45, (1956).

8. K. Yosida, Phys. Rev. 106, 893, (1957). 107, 396, (1957).

9. Frohlich and Nabarro, Proc. Roy. Soc. A175, 382 (1940).

10. A. B. Kaiser and S. Doniach, Intern. J. Magnetism, Vol. 1 p. 11-22, (1970).

11. M. P. Sarachik, Phys. Rev. 170, 679, (1968).

12. M. P. Sarachik, D. Shaltiel, J. Appl. Phys. 38, 1155, (1967).

13. Friedel, 'J. Suppl. Nuovo cimento 7, 287, (1958).

14. P. W. Anderson, Phys. Rev. 164, 352, (1967).

15. P. W. Anderson, Phys. Rev. 124, 41, (1961).

16. G. F. Koster and J. C. Slater, Phys. Rev. 96, 1208, (1954).

17. A. J. Heeger, 'Magnetic moment and non-moment' "Solid State Phys." Vol. 23, (1969).

18. D. Gainon and A. J. Heeger, Phys. Rev. Letters, 22, 1420, (1969).

19. J. W. Loram, R. J. White and A. D. C. Grassie, Phys. Rev. B, Vol. 5, (1972).

20. B. Grovanini, Phys. Letters, Vol. 31A, 2, 63, (1970).
H. Suhl, Phys. Rev. Letters, 20, 656, (1968).

21. Y. Nagaoka, Phys. Rev. 138, A1112-20, (1965).

22. H. Suhl, Phys. Rev. 138, A515-23, (1965).

23. P. Lederer and D. L. Mills, Phys. Rev. 165, 837, (1968).

24. A. D. Caplin, C. Rizzuto, Phys. Rev. Letters 21, 746, (1968).

25. A. D. Caplin, Phys. Letters 26A, 46, (1967).

26. B. R. Coles Phys. Letters, 8, 243, (1964).

27. J. Bardeen, L. N. Cooper, J. R. Schrieffer, Phys. Rev. 106, 162, (1957); 108, 1175, (1957).

28. J. Bardeen, 'Electron Vibration Interaction and Superconductivity', Rev. Mod. Phys. 23 261-270, (1951).

29. C. F. Ratto, A. Blandin, Phys. Rev. 156 513-21, (1967).

30. A. B. Kaiser, J, Phys. C3, 409, (1970).

Chapter Two

Apparatus and Methods of Experiment

2.1 Introduction

From the cryogenic view point, electrical resistivity and other quantities such as magneto-resistance, Hall effect, or superconductivity transition temperature measurements are among the properties whose measurement presents no great difficulties. These determinations require the entry of only a limited number of electrical leads into an isolated double can arrangement containing the samples, and are unaffected by the exchange of thermal energy with the surroundings; the specimens are kept in thermal equilibrium with a thermometer either by direct contact, by exchange gas, or by immersion of the samples and thermometer into a common refrigerating bath.

It has been noted that the slow drifts in temperature of the specimen and their surroundings do not directly affect seriously the determination as they generally do in Calorimetric or thermal conduction measurements, yet, they still introduce a small uncertainty as to the precise temperature of the samples at the particular times when measurements are made.

In this investigation the electrical resistance of metals or alloys in rod form is measured over a limited range of temperature —— from 1.46° K to room temperature —— by immersing the samples in a series of liquified gas refrigerants, which boil under controlled pressure. The gases we employed here in our experiment were nitrogen and helium of boiling points 77.° K and 4.21° K at normal pressure respectively.

2.2 Sample mounting

Alloys sample of different atomic concentration were prepared by melting together the appropriate proportions of the elements of interest, in an argon arc furnace under controlled pressure. Sets of up to five sample alloys of various atomic percentage compositions were made and then fashioned into thin specimens in rod form of reasonable lengths. Small form factors (the area to length ratios) A/L were required to yield reasonably high resistance values, typically 10^{-3} ohm.

The set of sample alloys, up to maximum of five, together with the pure host were mounted onto pairs of knife edge supports attached to a copper block, as indicated schematically in Figure (2-1).

Four # 2-32 bolts, a mylar insulating strip, and a thin brass yoke, held the ends of the samples in good electrical and thermal contact with knife edge supports. For the system of alloys we studied —— Cr and Fe in Ruthenium —— the production of long samples was hampered by the brittle nature of the Ruthenium, they required an addition to the mount-assembly[1].

To accomodate shorter samples without substantially altering the original positions of the knife edge supports, the idea of using "floating" knife edge supports was introduced, Figure 2-2, and used in the manner indicated in Figure 2-1a. The effective length L of the sample is the length between the knife edge supports. As "floating" knife edge supports were introduced in our sample assembly, the upper and lower fixed-points for effective length measurement were measured differently. Instead of measuring the knife edge to knife edge distance, a suitable reference point for each sample on the sample holder had to be chosen; usually we choose the edge of the gas thermometer bulb (see Fig.2-3)

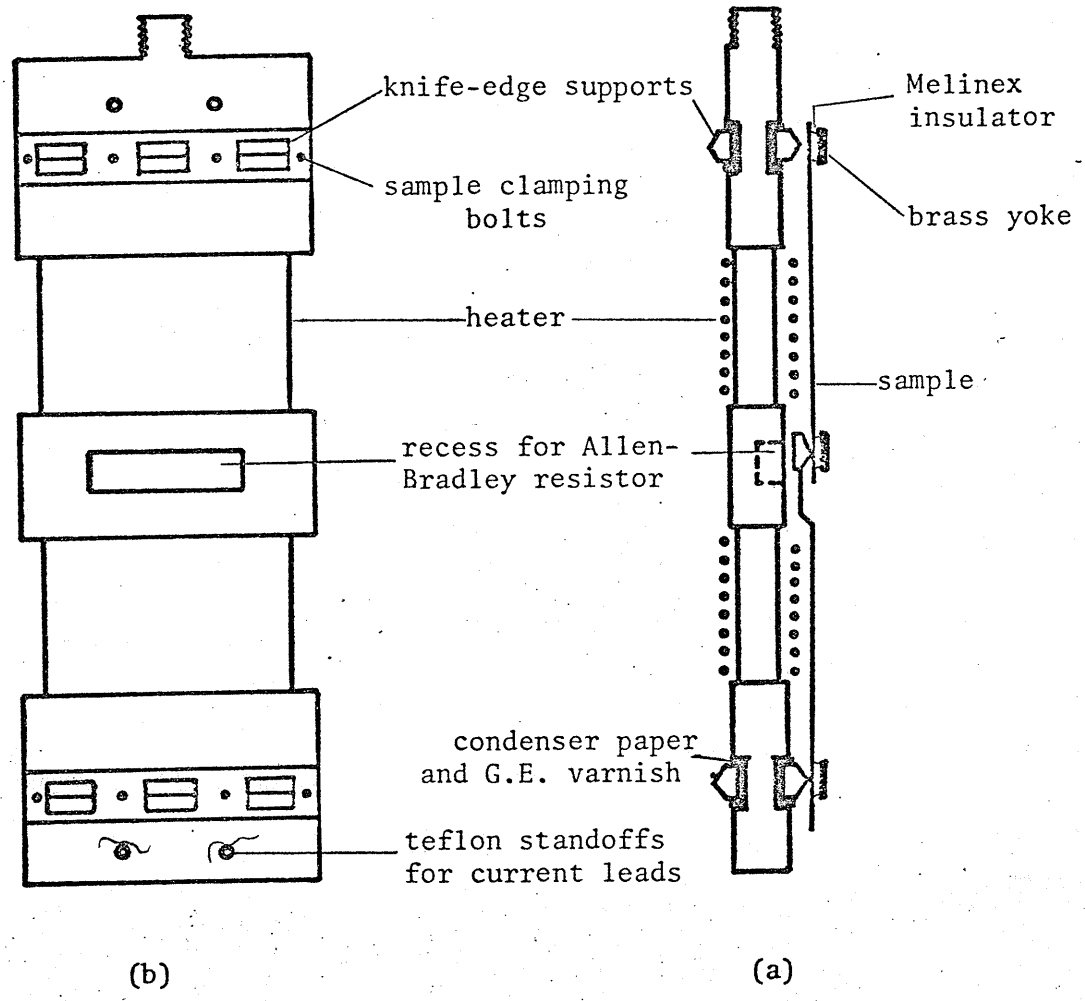

FIG.-2-1 (a) Edge-view of mounting block

(b) Face-view of mounting block

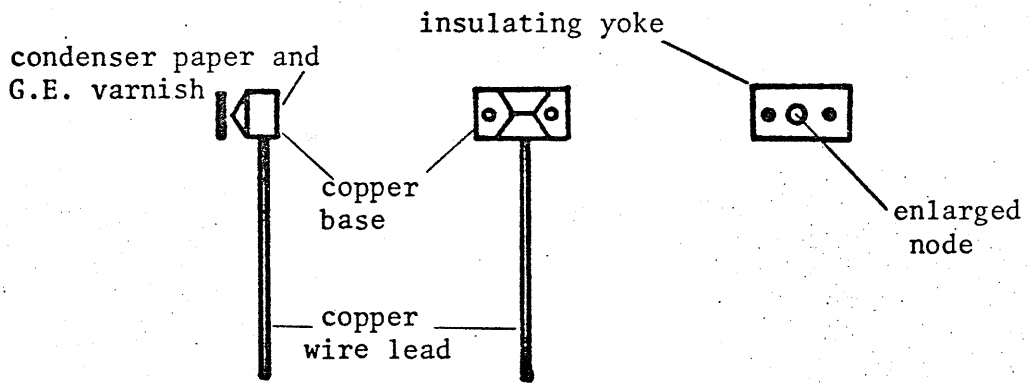

FIG.-2-2 Face-and edge-views of "floating" knife-edge supports.

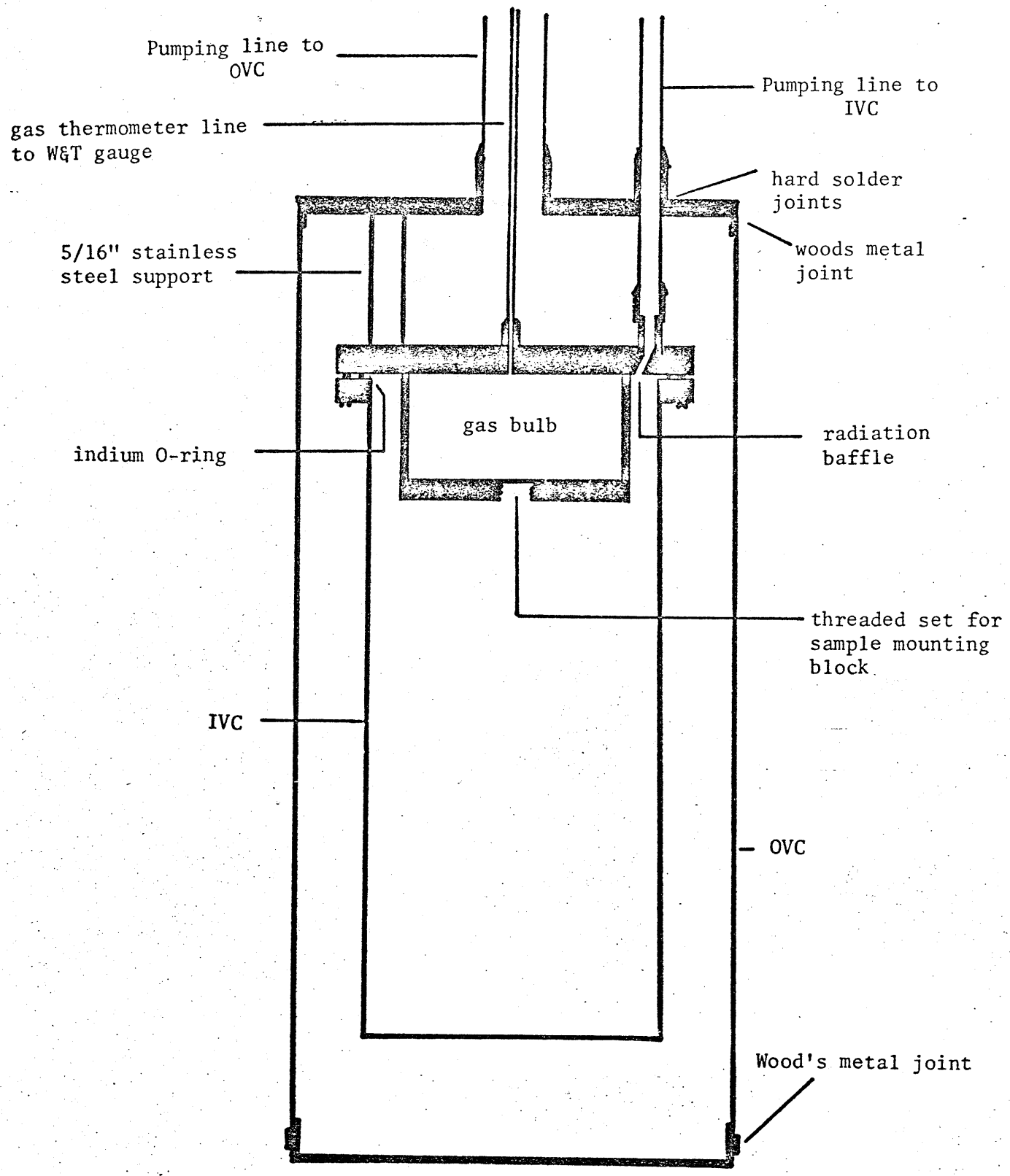

FIG.-2-3 Details Of The OVC, IVC And Gas Bulb.

immediately above the corresponding pair of knife edge supports. The distances from this chosen reference point to the upper and lower knife edges respectively were measured with the travelling microscope.

Measurements on the upper knife edges could be made easily before the mounting of the alloy samples. The use of "floating" knife edge supports, however, introduce some measurement difficulties. For this reason, bigger holes in the middle of the "yoke" of the "floating" knife edge supports were made so that knife edges would be viewed through these holes, and hence measurements could be made more accurately.

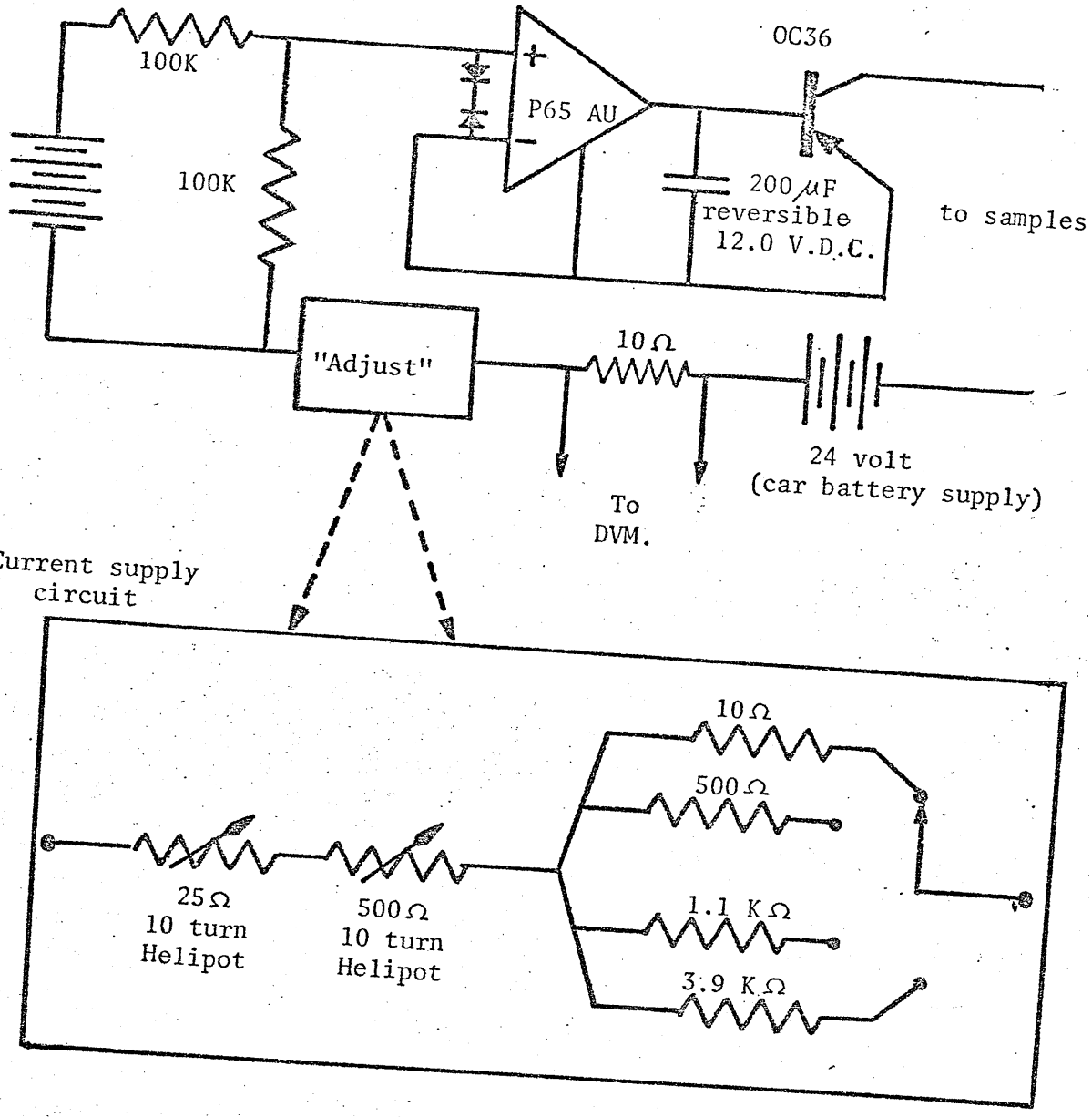

(a) Current supply circuit

FIG. 2-4 (b) Details of "Adjust" resistor

2.3 Resistance measurement

The resistances (and hence the resistivities) of the sample alloys are found using a simple DC technique. A highly stablized sample current was required and this was achieved by regulating an OC-36 transistor with a Philbrick P65 AU operational amplifier, FIG. 2-4. The voltages required to operate the operational amplifies were supplied by a fifteen volt bipolar power supply, FIG. 2-5. At the same time, separate Zener regulated supplies were used for reference voltage unit and current supply unit to avoid grounding problems.

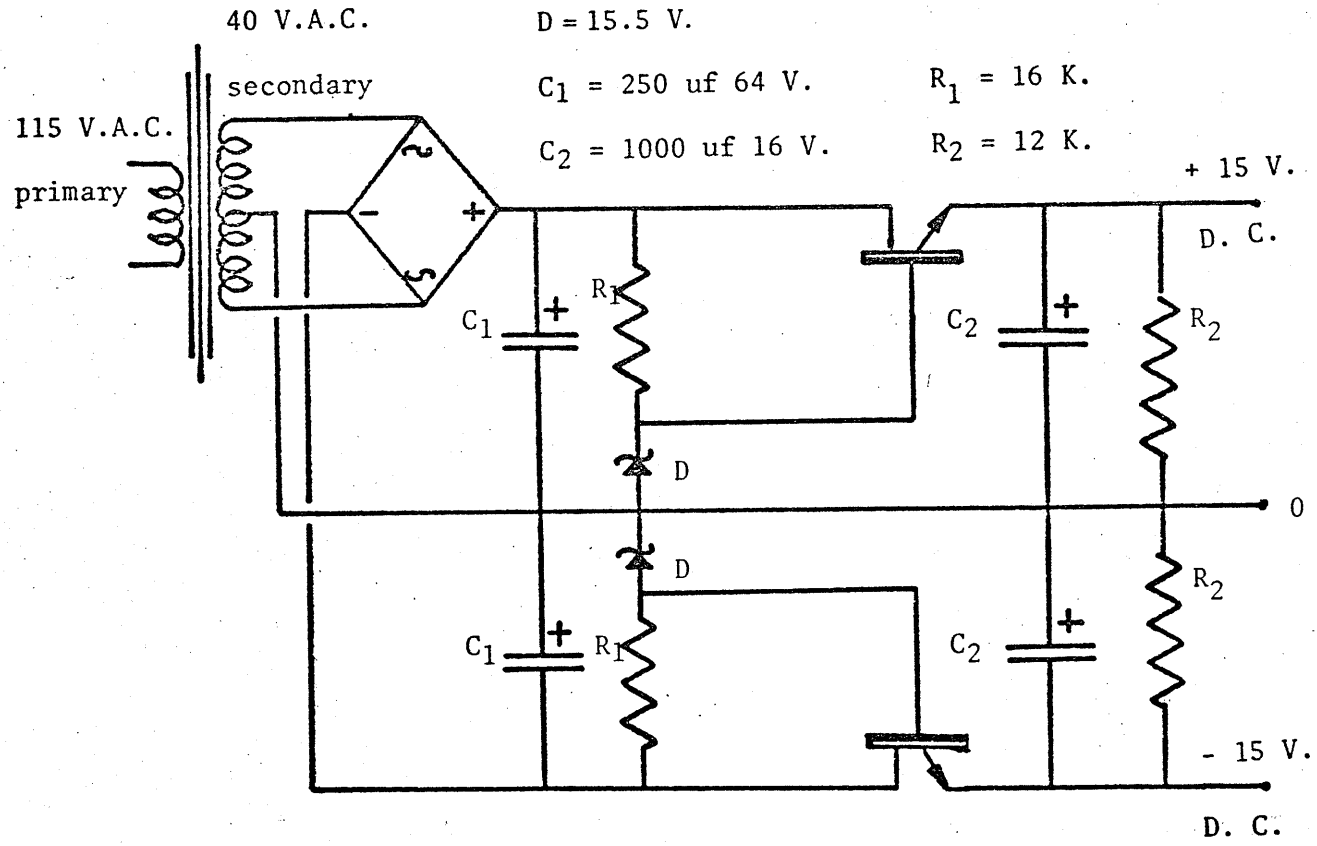

FIG.-2-5 Circuit Diagram Of Op. Amp. Power Supply

Voltage and current measurements were made on the samples by using a standard four probe technique[2]. Currents through the samples were varied to balance a highly stable reference voltage using a Kiethley-microvoltmeter as a null detector. Balance could be obtained to about $2. \times 10^{-9}$ V.

The sample current was found by measuring the voltage this current produced across a 10 ohms Muirhead standard resistor connected in series with the specimens. The potential drop across this resistor was measured with the D.V.M. with a resolution of about 1 part in 10^5, which gave 10 x I where I is the sample current. Both "forward" and "reverse" readings were taken, thus effects such as thermal voltage, would be cancelled out after averaging these two results. The voltage and current ratios for all specimens were found to be independent of the current over

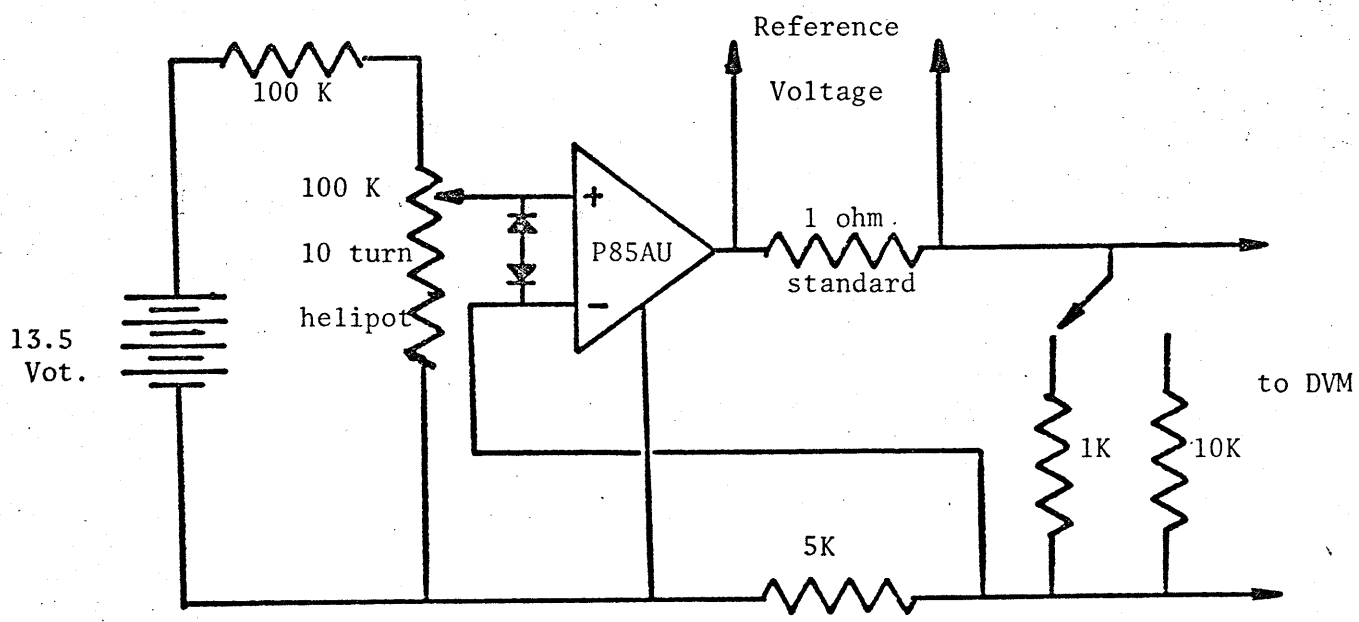

FIG.-2.6 Reference Voltage Supply Circuit.

the current range used, implying negligible joule heating effect.

The sample voltages were taken from a wire-wound standard one ohm resistor (Leeds and Northrup cannister type 29232, of 0.01%), supplied from a stabilized operational amplifier. Either a 1 K or 10 K ohm Muirhead (±0.02%) thermally stable standard resistor could be connected in series with this one-ohm resistor to generate a magnified voltage (to an order of 10^3 or 10^4 respectively) from which the voltage readings were taken by the D.V.M. The voltage supply circuit is shown in FIG. 2-6. Again, the actual sample voltage was found by averaging the forward and reverse readings from the D.V.M.

2.4 Temperature achievement, control and measurement

Since resistance as a function of temperature was being sought, an accurate means of varying and controlling the temperature was essential.

The sample holder block with samples was mounted inside a double can arrangement, as indicated in Figure (2-3). Temperatures of 4.21°K and below were obtained by surrounding this can with liquid helium, boiling at controlled vapour pressure, (the outer dewar was filled with liquid nitrogen at this stage)[3]. The complete picture can be understood better with the block diagram shown in Figure (2-7). Temperature points below 4.2° K were obtained by pumping on the liquid helium in the inner dewar, and were stablized with a manostat in the He pumping line. The lowest temperature we could achieve would be about 1.46° K. When the pressure of helium in the inner dewar was in the range 76 cm to 3 cm. Hg, temperature measurements were made by measuring this pressure on a mercury manometer. When the helium pressure was below 3 cm. Hg, an oil manometer was used for higher accuracy.

The corresponding temperature were found by linear interpolation between listed vapour pressure-temperature points extracted from "Experimental techniques in Low temperature Physics" by G. K. White[4]. Temperature measurements were accurate to five millidegrees.

Temperature above 4.2° K was obtained by slowly heating up the sample holder block, and hence the sample, with a heating coil wound around the sample mounting block. Temperatures were controlled with this heating coil connected to a feed-back circuit, FIG. 2-8. —— an A-C phase-sensitive Wheatstone Bridge with a rectified D-C feedback current to the heater. Temperatures of the sample block were roughly estimated by an Allen-Bradley carbon resistor of 100 ohms normal value, seated at

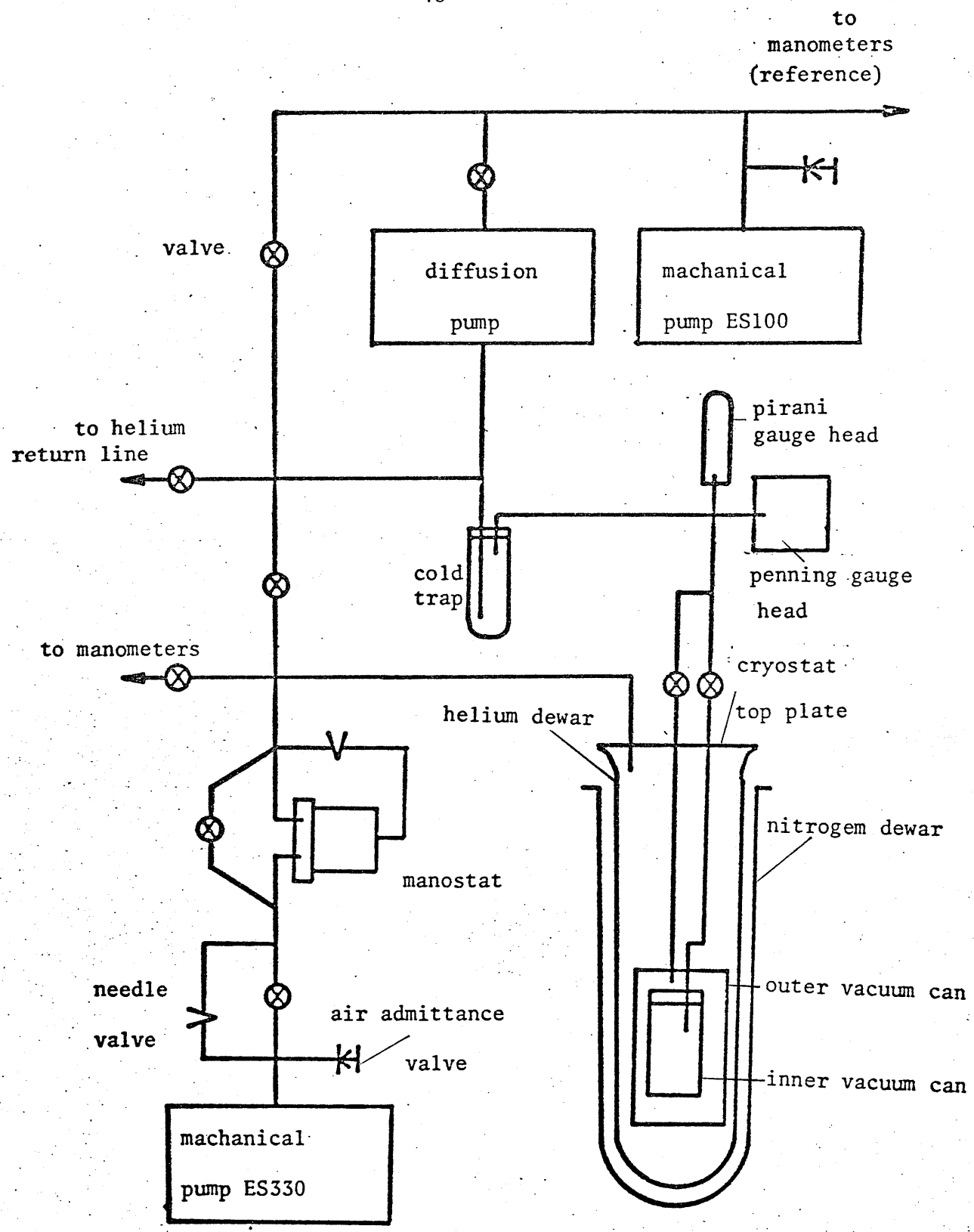

FIG.-2-7 Block Diagram Of The Vacuum System

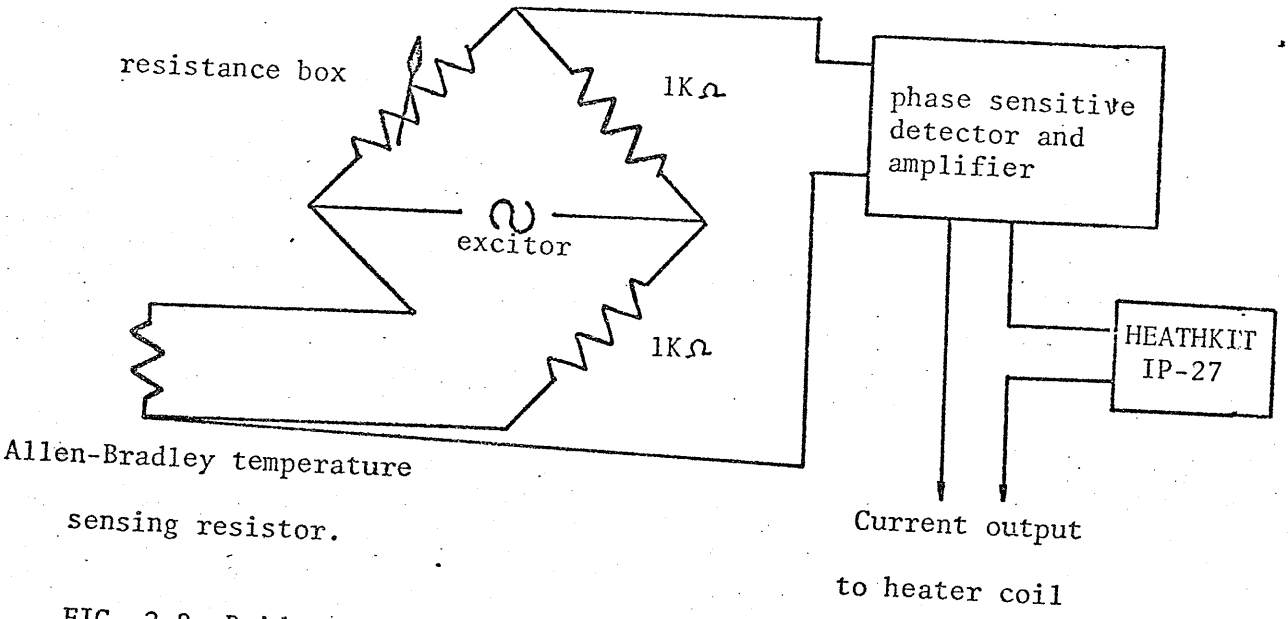

FIG.-2-8 Bridge circuit. Note the three leads to the Allen-Bradley to balance the lead resistance.

the centre of the sample block. The resistance of this carbon resistor increases roughly logarithmeatly with decreasing temperature, FIG. 2-9. Accurate temperature measurements above 4.2° K were made with a non-linear gas thermometer. The temperature pressure relationship for this gas thermometer arrangement is given by:-

$$P\left[\frac{V_B}{T} + \frac{V_L}{T_R - T} \ln \frac{T_R}{T} + \frac{V_o + bP}{T_R}\right] = k \qquad (2.1)$$

where the constant k was evaluated by using the known filling temperature and pressure T_o and P_o (usually, either the ice point values or the helium temperature values were used). For our experimental arrangement the characteristic values in Equation (2,1) have the following values.

V_L —— Volume of the Cryostat tubes = 0.0130 in^3, this value might drop about 1.% from room temperature to 77° K in our system.

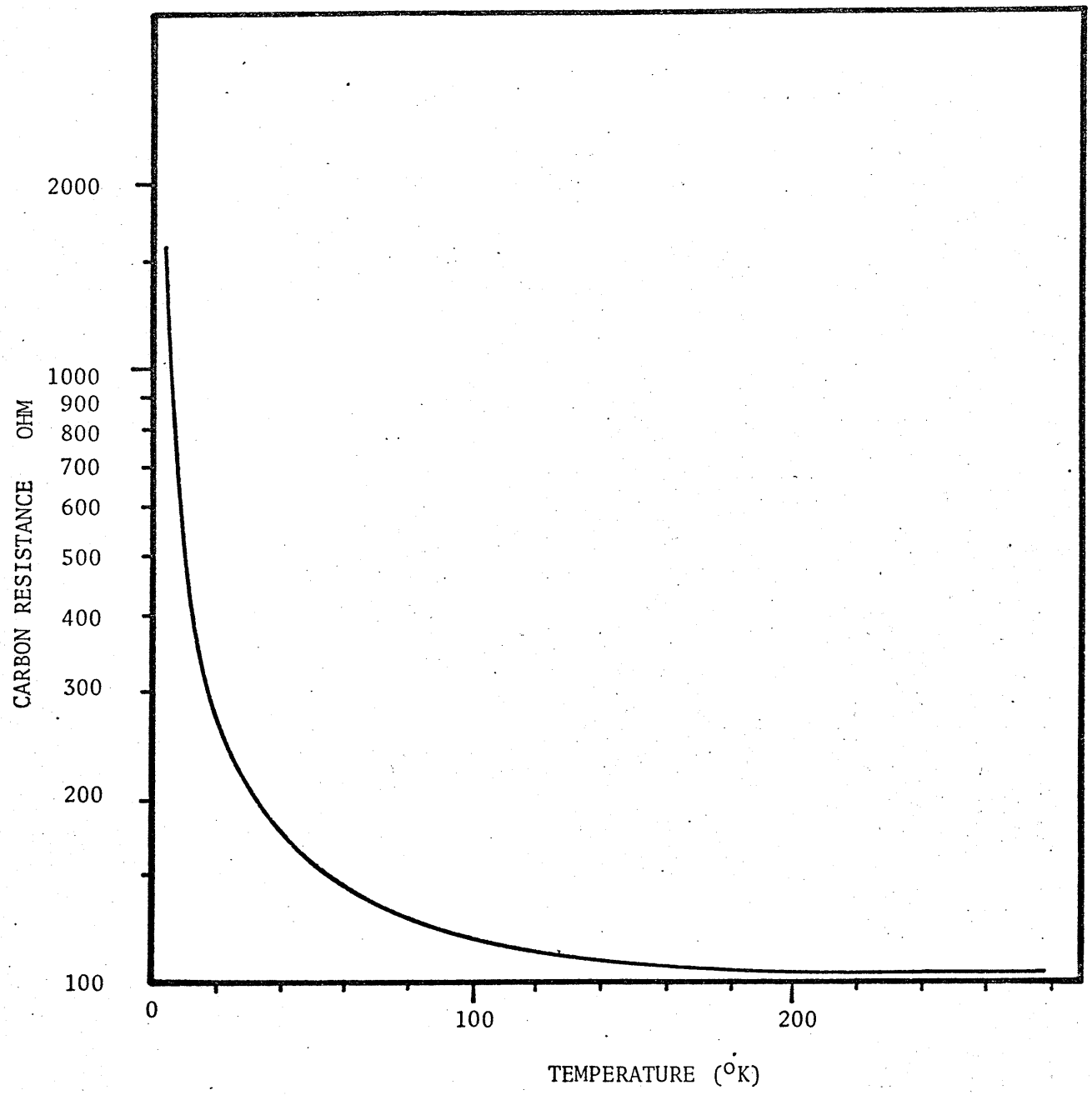

FIG.-2-9(a) Resistance Verses Temperature Characteristics Of The Allen-Bradley Resistor

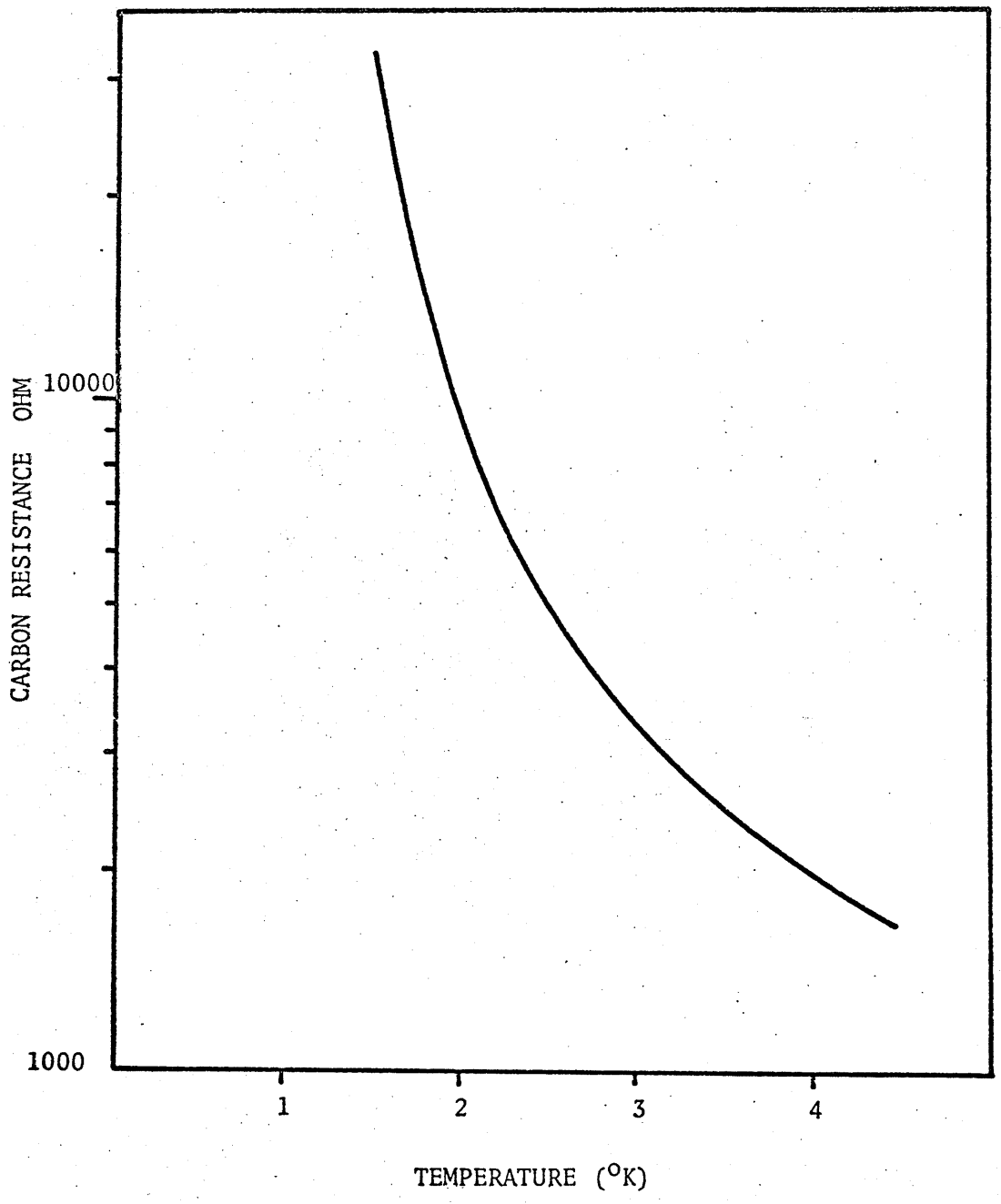

FIG.-2-9(b) Resistance Verses Temperature Characteristics Of The Allen-Bradley Resistor Below 4.5° K

V_o —— the pressure independent portion of the volume associated with connecting tubes at room temperature = 1.18 in^3.

V_B —— the volume of the gas bulb sitting on top of the sample block

= 1.497 in^3 at room temperature

= 1.481 in^3 at liquid nitrogen temperature

= 1.480 in^3 at liquid helium temperature

b —— the Wallace and Teernan pressure gauge constant = 0.00115 in^3 per inch water pressure.

The corresponding temperature readings for a given gauge pressure reading was obtained by computer calculation. Further corrections were made in light of the non-ideality of helium gas (due to mainly Van der Waal type interaction), using interpolations from a set of Virial coefficients[5].

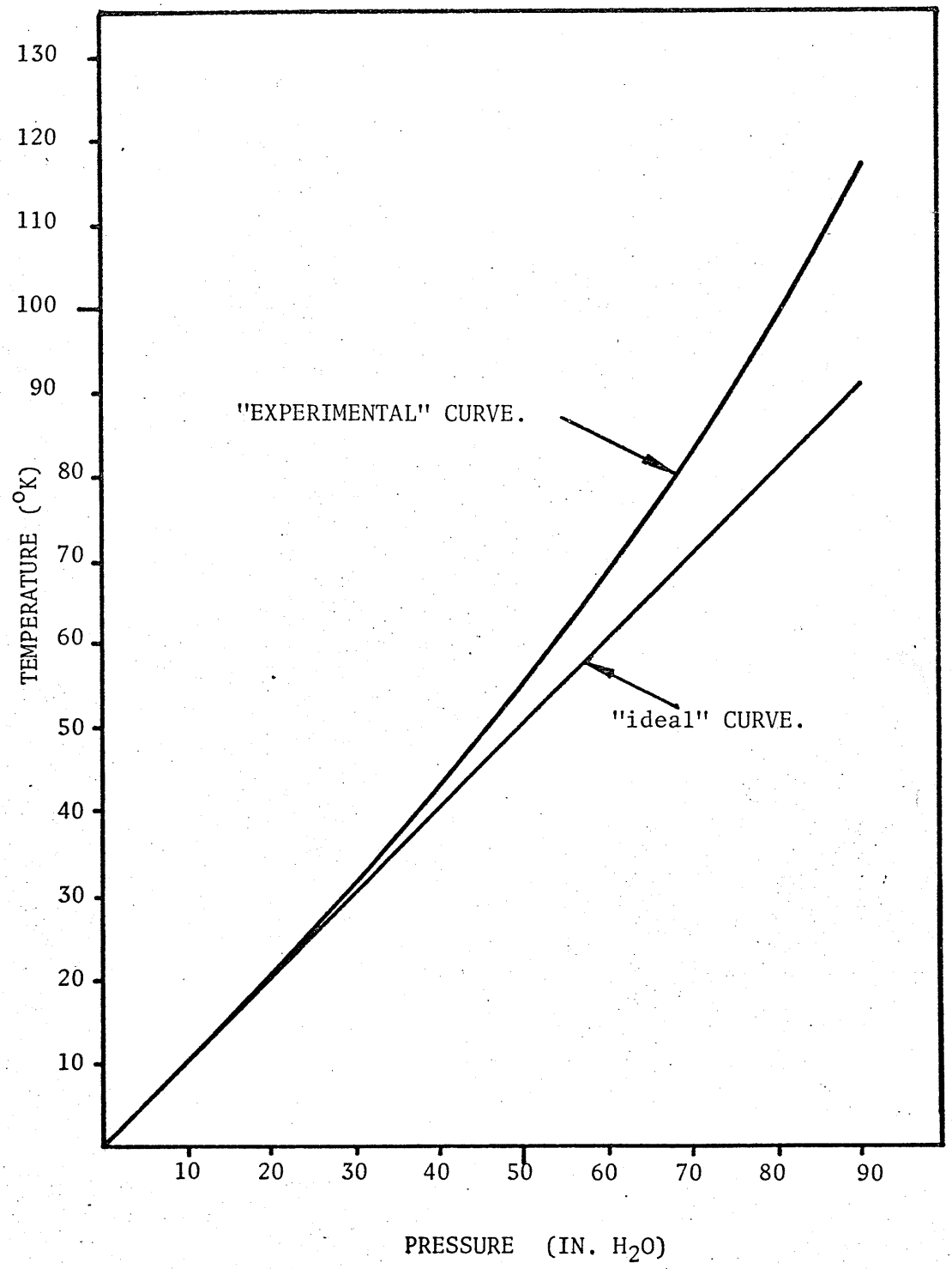

FIG.-2-10 NON-LINEARITY OF THE GAS THERMOMETER FOR THE CASE

$T_o = 4.2\ ^oK$ $P_o = 4.35$ IN. OF H_2O

2.5 Reference

(1) M. E. Colp "Transport Measurements On Some Dilute Alloys Pd-Co, and Ru-Mn", Thesis Un. of M. (1972) unplished.

(2) A.D.C. Grassie, G. A. Swallow, Gwyn Williams, and J. W. Loram Phys. Rev B3 4154 (1971)

(3) K. Mendelssohn "Cryophysics" Interscience Pub. L.T.D. London 1960

(4) G.K. White "Experimental Techniques in Low Temperature Physics" Second Edition, Oxnard 1968

(5) W. H. Keesom "Helium" Elsevier, Amsterdam, k942

Chapter Three

Dilute Alloy Systems Ru Cr., and Ru Fe.

3.1 Introduction

The properties of dilute alloys have been studied quite extensively during the last twenty years. We presently examine the low temperature resistivities of some Ru Cr and Ru Fe Alloys. Recently, Riblet and Jensen studied the superconducting transition temperature, Tc, for a number of Ruthenium based alloys, and found that the rates of decrease of Tc with impurity concentration c, dTc/dc for the "magnetic" impurity alloys Co[1] and Fe[2] were more rapid than that for the "non-magnetic" impurities, Ni, Rh, Ir, Pt and Pd. These authors, furthermore, noted that this rapid decrease in superconducting transition temperature Tc was explicable as the basis of d-level spin fuctuations localized within the impurity cell. Chromium and iron, used as impurities in dilute alloy studies, in fact show well defined magnetic behaviour in Au Cr[3] and localized spin fuctuation effects in Al Cr[4], Pd Cr[5], Pt Fe[6] and Pt Cr[7], and this stimulated our interest in investigating the dilute Ru Cr and Ru Fe alloys.

Manganese, used as an impurity in dilute alloys, also shows well-defined magnetic behaviour as in Pd Mn[8] and Au Mn[9] and ℓsf effects in Rh Mn[10] and Al Mn[3].

3.2 Experimental Details

The samples were prepared from 99.999% pure Ru sponge, 99.999% pure Cr beads, and 99.9985% pure Fe rod, all supplied by Johnson Matthey and Co., London, U.K.

Metallic Ru was produced by pressing the Ru sponge in a hardened stainless steel dye, and melting the resulting pellets together on the water cooled copper hearth of an argon arc furnace, incorporating a tungsten electrode and a titanium getter. Ru solidifies into an hcp structure with a c/a ratio considerably less than "ideal", and is thus very difficult to cold roll into a suitably shaped resistance specimen. As a result, the Ru was cast into a long cylindrical trough of approximate diameter 7 mms, producing a sample of cylindrical form and approximately 4 to 7 cms long.

Master Ru Cr and Ru Fe alloys, containing about 10 at. % Cr and Fe respectively, were prepared by melting the appropriate amounts of the metals together in the arc furnace. Both alloys were homogenised by inverting and remelting several times; melting losses were negligibly small. Ru Cr alloys containing normally 0.2, 0.4 and 0.8 at. % Cr, and Ru Fe alloys of nominal Fe concentration 0.4, 0.8 and 1.0 at. %, were prepared by dilution. Resistivity specimens, with a square cross-sectional area of about 2.5×10^{-3} sq. cm were then cut from these cylindrical samples using a diamond saw.

The form factors (area to length ratio) were determined using a method described by Loram, Whall adn Ford[11]. The knife-edge to knife-edge distance of the sample supports (potential contacts) can be measured accurately with the travelling microscope (discussed in section 2.2). The density of each sample is determined from lattice spacing data, using the formula

$$\text{Density} = \frac{2 \cdot 3}{N\, a^2\, c} (A_1 X_1 + A_2 X_2) \qquad 3.1$$

where N is Avogadro's number, A_1 and A_2 are the atomic weights of the elements used, X_1 and X_2 being their respective fractional atomic compositions, and the factor 2 indicates that there are two atoms per unit cell in the h.c.p. ruthenium. The "a" is the concentration dependent lattice constant of the alloy. Bozorth et al[12] show that in the concentration range under study, Vegard's Law[13] is applicable. The lattice constants are obtained from the law in conjunction with the lattice spacing of pure Ru (a = 2.6987 Å, c = 4.2811 Å), pure Cr (2.8839 Å) and Fe (2.8607 Å).

From the density, and an accurate measurement of the sample weight (±0.1 m gm.), the volume of the sample is determined. The travelling microscope is again employed to find the exact length of the specimen which, with the volume, readily yields the average cross-sectional area. Making the portions of the specimen which over hang the knife-edge as short as possible, minimizes the error in the mean cross-sectional area between the knife-edges. The ratio of the cross-sectional area to the inter-knife-edge spacing yields the required form factor for the specimen. Tables 3.1 and 3.2 list respectively the computed lattice constants, form factors, and inter-knife-edge spacing for the Ru Cr and Ru Fe system used.

These specimens were subsequently etched in warm dilute acid of the following composition,

1/5 Volume of water

1/5 Volume of concentrated nitric acid

3/5 Volume of hydrochloric acid and

a good splash of hydrogen peroxide, and annealed in vacuo for 30 hrs. at $1000^{o}C$.

The resistance of these samples was measured, using a four probe technique in which the current through each sample was varied to produce a balanced against a highly stable voltage. The estimated accuracy of resistance measurement is about 2 parts in 10^4 (Grassie et al, 1971[14]). Temperatures below 4.2^{o} K were stabilized and measured to ±5 m deg., and finally, those above 4.2^{o} K to better than 1.% using a non-linear gas thermometer.

Table 3.1

Summary of the Physical Quantities of Ru Cr Alloys

Concentration (at. % Cr)	Lattice constant a (Å)	Cross-section Area (sq. cm) ±0.001	Effective * length (cm) ±0.001	Form factor (cm)
Pure Ru	2.6987	4.712×10^{-3}	4.341	1.105×10^{-3}
0.2	"	2.468×10^{-3}	2.450	9.983×10^{-4}
0.4	"	3.612×10^{-3}	5.495	6.603×10^{-4}
0.8	"	3.021×10^{-3}	3.503	8.697×10^{-4}

* Inter-knife edges spacing

Table 3.2

Summary of the Physical Quantities of Ru Fe Alloys

Concentration (at. % Fe)	Lattice constant a (Å)	c/a ratio	Cross-section Area (sq. cm) ±0.001	Effective * length (cm) ±0.001	Form factor (cm)
0.4	2.7050	1.5823	4.216×10^{-3}	4.987	8.557×10^{-4}
0.8	2.7045	1.5824	7.032×10^{-3}	2.866	2.479×10^{-3}
1.0	2.7040	1.5825	4.184×10^{-3}	2.080	2.208×10^{-3}

* Inter-knife edges spacing

3.3 Results and Discussion

(i) Pure Ruthenium

The temperature dependence of resistivity of Ruthenium has been studied quite extensively. It has been found that resistivity of single crystals of Ruthenium depends on orientation[14,15], the difference between the resistivity measured parallel and perpendicular to the c axis being about 10% at room temperature.

The pure Ruthenium used in our investigation had an electrical resistivity ratio ($\rho(297^{o}K)/\rho(1.45^{o}K)$) of 123 with $\rho^{i}(297^{o}K) = 7.33 \pm 0.08\,\mu\Omega$cm. which is close to the value of the resistivity for polycrystalline close-packed hexagonal Ruthenium.

Figure 3.1 shows the plot of the temperature dependent part of pure Ruthenium electrical resistivity

$$\rho^{i}(T) = \rho(T) - \rho(T = 1.45^{o}K) \qquad 3.2$$

against temperature. Because the uncertainties in the measured $\rho(T)$ constitute a considerable propertion of $\rho^{i}(T)$ at temperature below $30^{o}K$, no data below this temperature are plotted in this figure; and, it is clearly impossible to observe the low temperature electron-electron scattering contribution to $\rho^{i}(T)$[14,16]. Within the temperature range from $30^{o}K$ to $60^{o}K$. Figure (3.1) indicates that $\rho^{i}(T) \propto T^{n}$; $n = 4.75 \pm 0.005$ which is in good agreement with the data obtained by White and Woods[16] (1959).

Figure 3.1

The thermal part of the pure Ru electrical resistivity; $\rho_T(T) = \rho(T) - \rho(1.45)$

The line drawn has a slope of 4.75±0.005

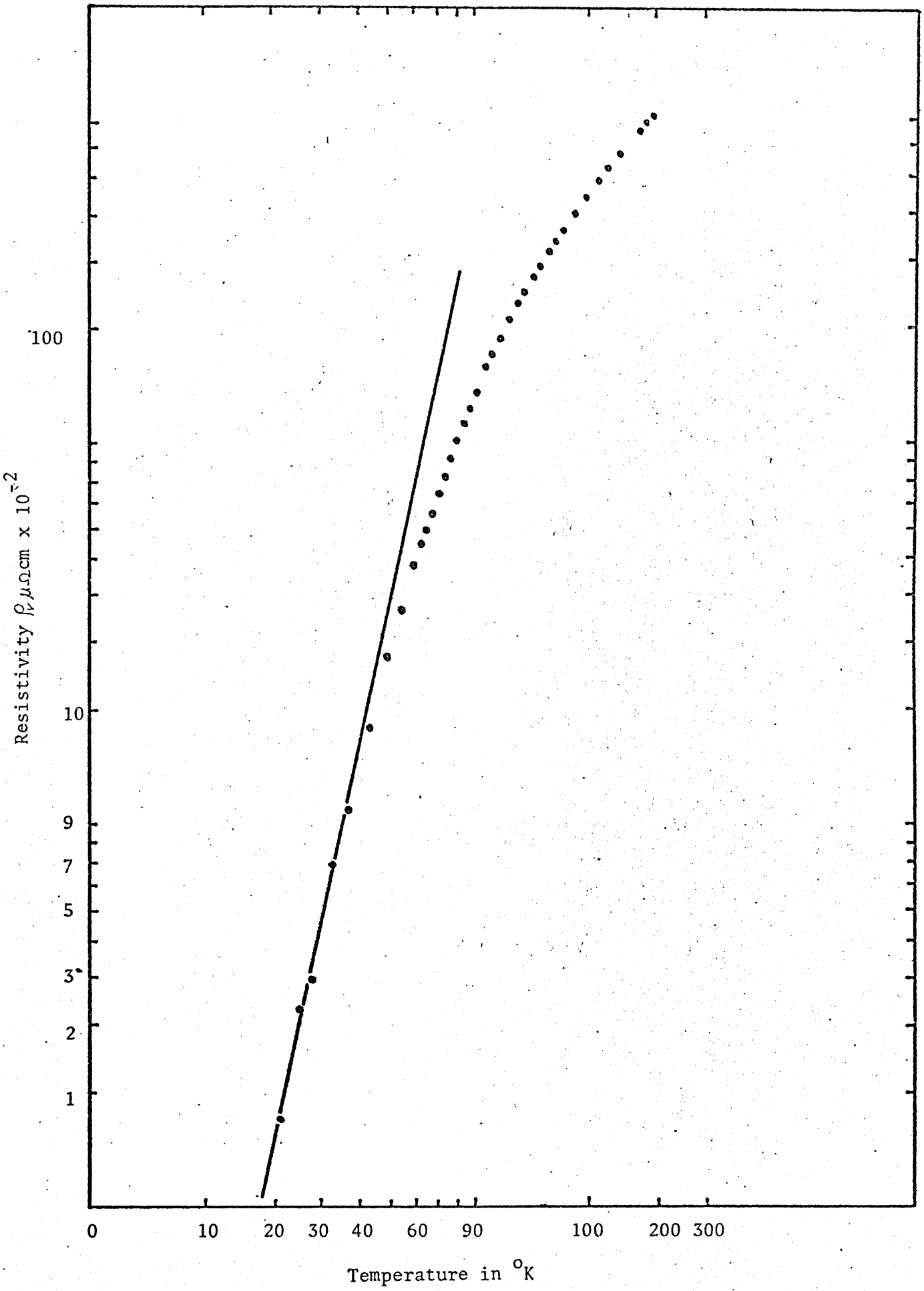
100
10
9
7
5
3
2
1
Resistivity $\rho_\nu \mu\Omega$cm x 10^{-2}
0
10
20
30
40
60
90
100
200
300
Temperature in ^{o}K

(ii) Ruthenium Chromium Alloys

The experimental data resulting from our measurements on Ru Cr alloys are shown in Figure (3.2) in which resistivities of alloys containing 0.8, 0.4 and 0.2 atomic percent Cr and of the pure Ru sample are plotted against temperature over the range from 1.45° K to 140° K. Close examination on Figure (3.2) reveals that the resistivities increase linearly with temperature above 75° K and are constant below 30° K. Figure (3.3) shows the plot of incremental resistivities

$$\Delta\rho(T) = \rho_{Alloy}(T) - \rho_{Ru}(T)$$

against temperature up to 140° K and from this figure, the incremental resistivities of specific impurity concentrations at absolute zero can be extracted; these are listed in Table (3.3). As shown in Figure (3.3), the temperature independence behaviour of $\Delta\rho(T)$ below 30° K implies that Cr impurities in Ruthenium are non-magnetic in the static Hartree Fock[17] (Friedal - Anderson) sense; this behaviour is a result of a spin independent conduction electron scattering cross-section at the impurity sites. At temperatures between 30° K and 75° K, a small increase, which depends slightly on impurity concentration, in $\Delta\rho(T)$ is observed. Such a phenomenon is the result of the competing effects of phonon and impurity scattering with presumably differing anisotropies[18], and this results in the break down of Matthiessen's Rule for the Ru Cr alloy system. An attempt to fit these deviations on the basis of a "Two Current" model was made; the latter yields[19]

$$\Delta\rho(T) - \Delta\rho(0) = \frac{\beta\alpha\,\rho_{Ru}^{i}(T)\,\Delta\rho(0)}{\alpha\,\rho_{Ru}^{i}(T) + \beta\,\Delta\rho(0)} \qquad 3.3$$

Figure 3.2

The resistivity $\rho_f(T)$ plotted against temperature (in ^{o}K) over the range from 0^{o} K to 140^{o} K, for the four specimens of Ru Cr alloys.

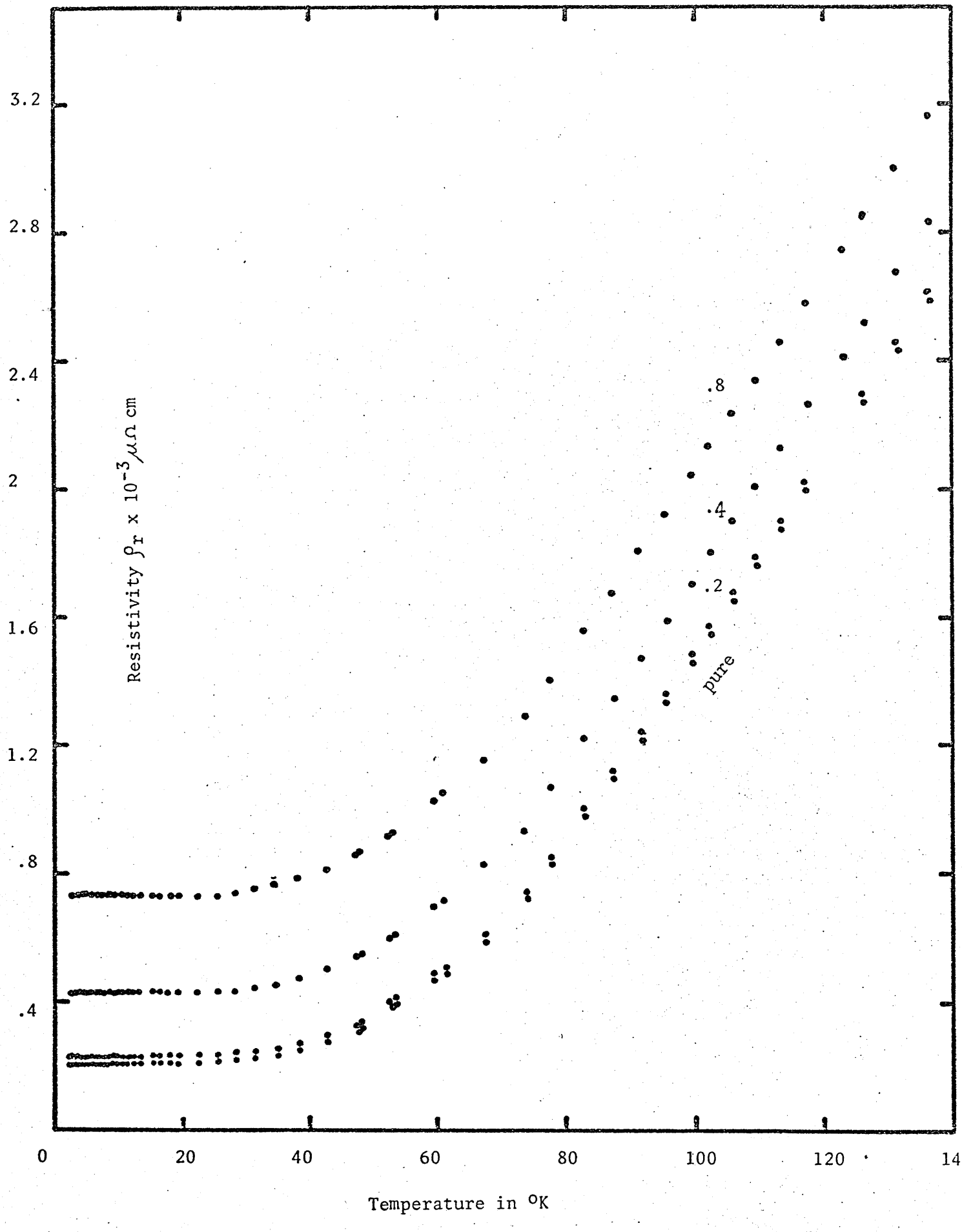
3.2
2.8
2.4
2
1.6
1.2
.8
.4
Resistivity ρ_r x 10^{-3} $\mu\Omega$ cm
.8
.4
.2
pure
0
20
40
60
80
100
120
14
Temperature in °K

Table 3.3

Summary of Data on the Ru Cr Alloys

Concentration (at. % Cr)	$\Delta\rho$(T = 0) ±0.005 $\mu\Omega$cms	$\Delta\rho$(T = 298° K) ±0.005 $\mu\Omega$cms
Pure Ru	0.060	7.38
0.2	0.114	0.125
0.4	0.213	0.242
0.8	0.515	0.524

Figure 3.3

The incremental resistivity of Ru containing 0.2, 0.4, and 0.8 at. % Cr plotted against temperature. The curve drawn are fits to Matthiessen's rule breakdown based on a two current model.

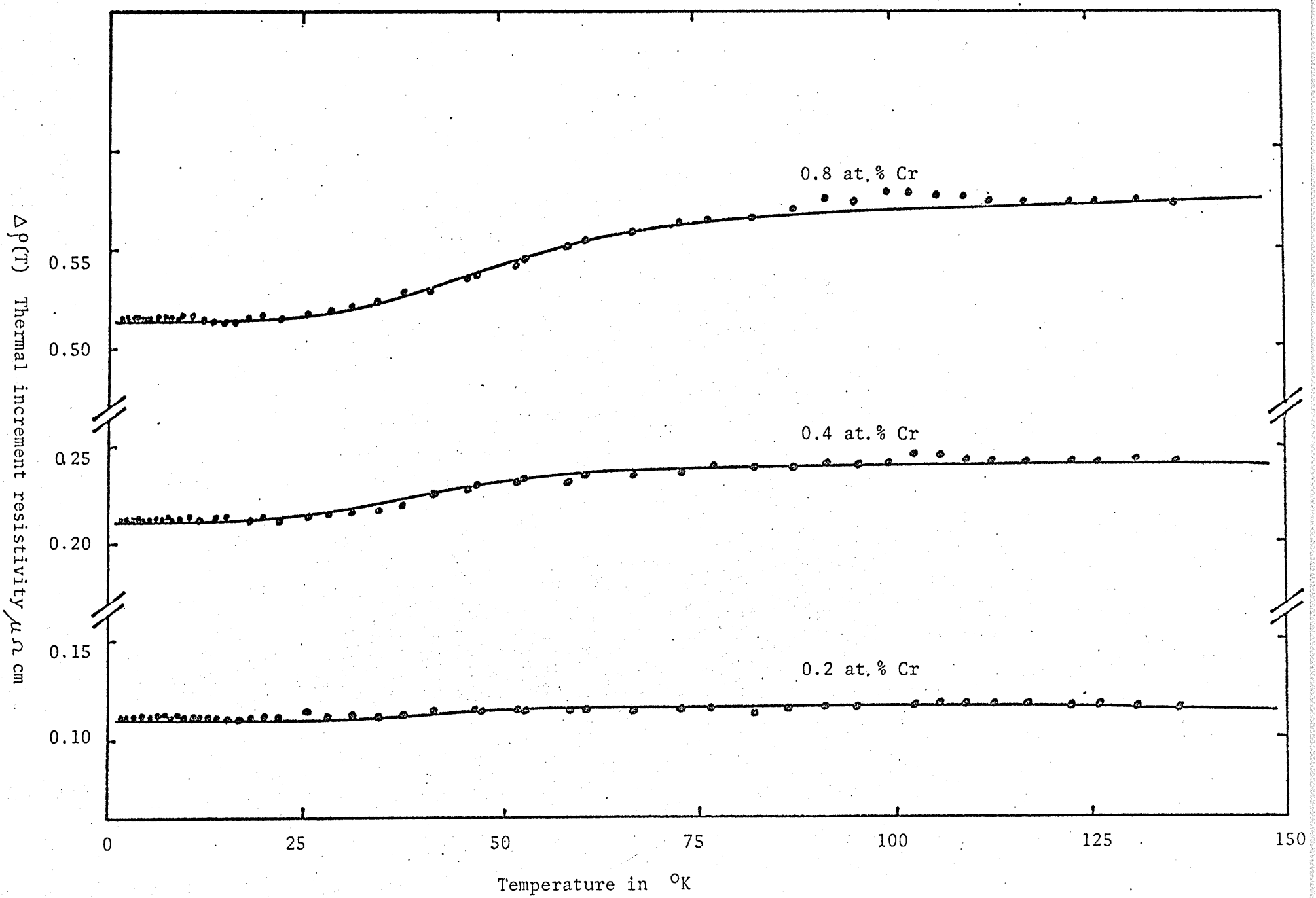
0.8 at.% Cr
0.4 at.% Cr
0.2 at.% Cr
0.55
0.50
0.25
0.20
0.15
0.10
0
25
50
75
100
125
150
Δρ(T) Thermal increment resistivity μΩ cm
Temperature in °K

where α and β are regarded as adjustable parameters for different systems. The solid curves in Figure (3.3) represent a fit of Equation (3.3) to the data; within experimental error, the data can be fitted with constant values of = 0.375 and = 0.123. These values for and are close to those estimated for Pd based alloys studied by Kao and Willians[20] (1973).

The listed values of $\Delta\rho(0)$ in Table (3.3) were plotted against impurity concentration c in Figure (3.4), which shows a symmetric variation of $\Delta\rho(0)$ with Cr concentration.

In fact, $\Delta\rho(0)$ = 0.61 ± 0.02 $\mu\Omega$ cm/at. % Cr.

Figure 3.4

The incremental resistivity at zero temperature $\Delta\rho(T = 0)$ for Ru Cr Alloys plotted against the Cr concentration. The line drawn has a slope of 0.61 $\mu\Omega$ cm per atomic percent Cr.

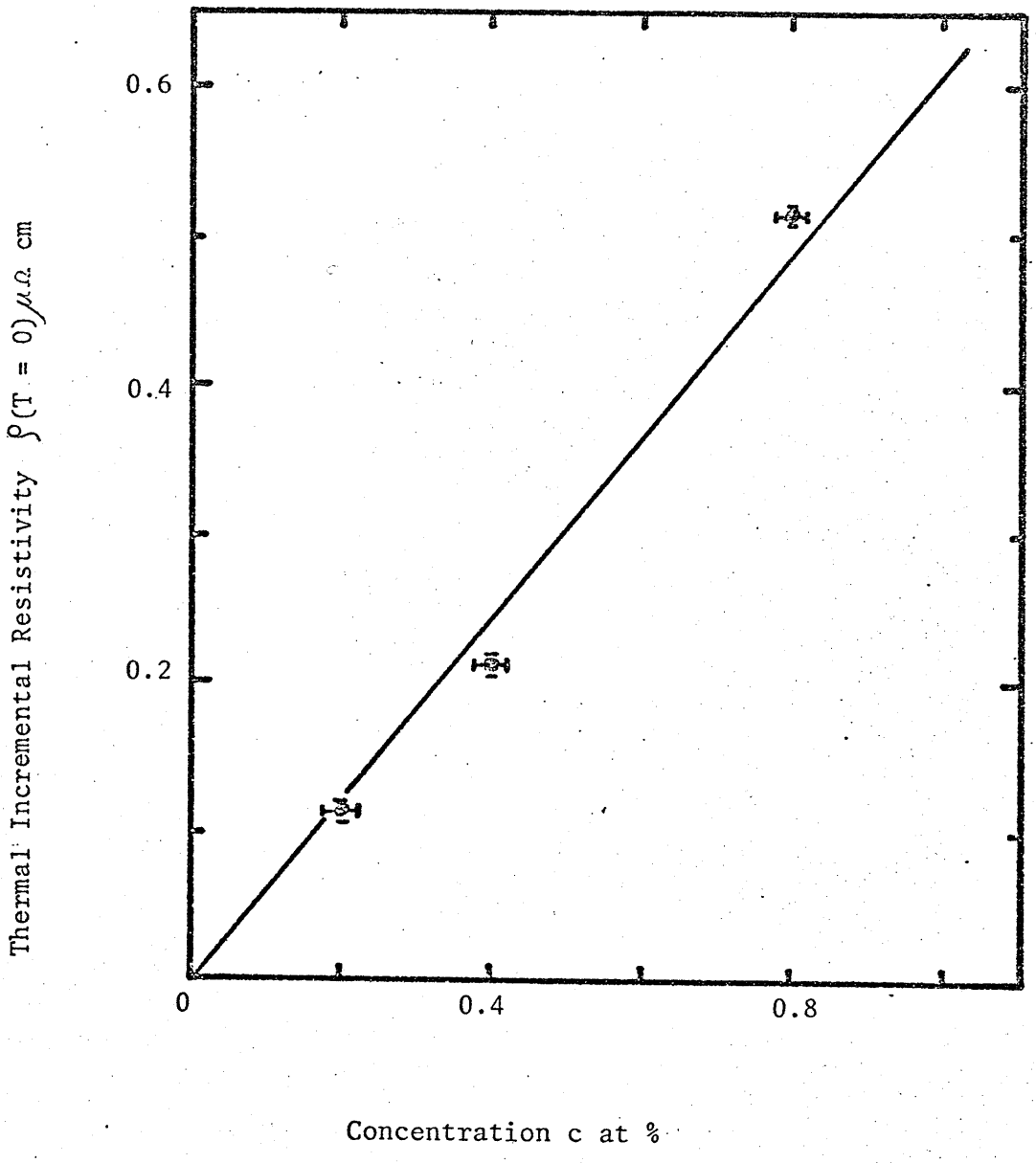
Thermal Incremental Resistivity $\rho(T = 0)\mu\Omega$ cm
0.6
0.4
0.2
0
0.4
0.8
Concentration c at %

(iii) Ruthenium Iron Alloys

The electrical resistivity of Ru Fe alloys was measured between 4.2 and 300K and the experimental results are summarized in Table (3.4). The listed incremental resistivity $\Delta\rho(T = 0)$ at absolute zero temperature indicates that this is a nearly isoelectronic system. A plot of the $\Delta\rho(T = 0)$ against impurity concentration in Figure (3.5) gives a slope of $0.14 \pm 0.02 \mu\Omega$ cm/at. % Fe.

Figure (3.6) shows a plot of the temperature dependence of the incremental resistivity $^{o}(T)$ over the range from $1.45^{o}K$ to $140^{o}K$. This figure shows that $^{o}(T)$ clearly rises more rapid in the 1.0 at.% Fe then in pure Ru. This result indicates a temperature dependent contribution to the total resistivity from the Fe impurities, and attention is now directed to find a model which might explain the observed behaviour.

The temperature dependent part of incremental resistivity

$$\Delta(T) = \Delta\rho(T) - \Delta\rho(0)$$

for 0.8 and 1.0 at % Fe alloys is plotted against temperature in Figures (3.7) and (3.8) respectively. The error bars in these Figures represent the effect of ± 1.% form factor uncertainty for each sample. A close examination of these figures shows that at temperature below $170^{o}K$ the thermal part of the incremental resistivities increase as T^2, becoming less rapid at higher temperatures. This is exactly the temperature dependent behaviour obtained by Kaiser and Doniach[20], (1970) and Rivier and Zlatic[21a,b] (1972). They concluded that this behaviour resulted from conduction electrons being scattered by localized spin fluctuation at the impurity sites. The former authors derived the following resistivity-

Table 3.4

Summary of the Data on the Ru Fe Alloys

Concentration (at. % Fe)	$\Delta\rho(T = 0)$ $\mu\Omega$ cms ± .1%	$\Delta\rho(T = 297)$* $\mu\Omega$ cms ± .1%	T^2 coefficient $10^{-6}\mu\Omega$ cm/K^2
0.4	0.053	0.13	2.5
0.8	0.115	0.37	6
1.0	0.140	0.42	7

* The quoted errors in this column result from the ±1.% shape factor error on each sample.

Figure 3.5

The thermal part of resistivity $\Delta\rho$ (T) = ρ(T) - ρ(0) plotted against temperature (in ^{o}K) over the range from 0^{o}K to 140^{o}K for 1.0 at. % Fe and pure Ru.

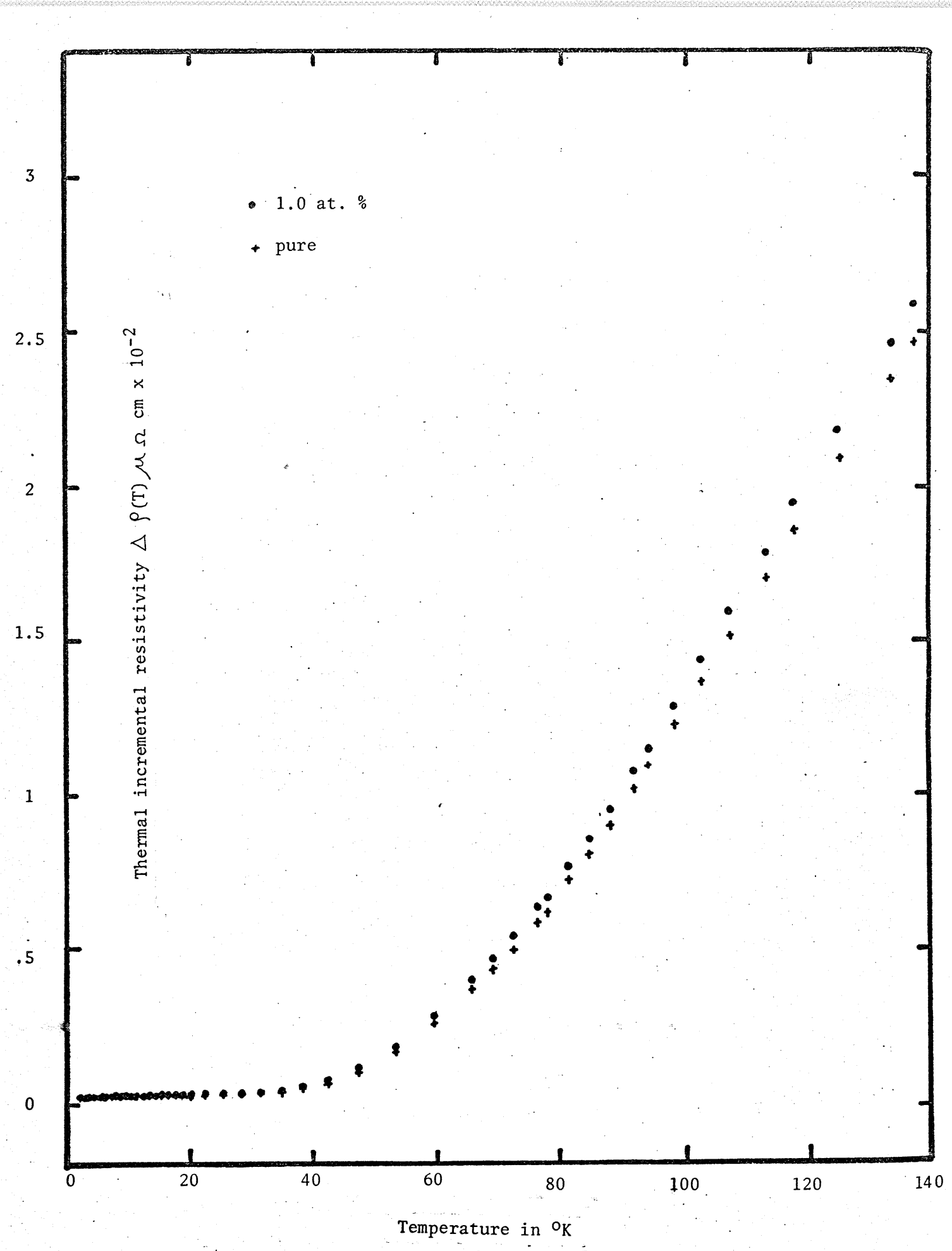
1.0 at. %
pure
Thermal incremental resistivity Δ ρ(T) / μ Ω cm x 10⁻²
3
2.5
2
1.5
1
.5
0
0
20
40
60
80
100
120
140
Temperature in °K

Figure 3.6

The thermal part incremental resistivity $\Delta(T = 0)$ for Ru Fe alloys plotted against the Fe concentration. The line drawn has a slope of 0.14 ± 0.02 $\mu\Omega$ cm/at.% Fe.

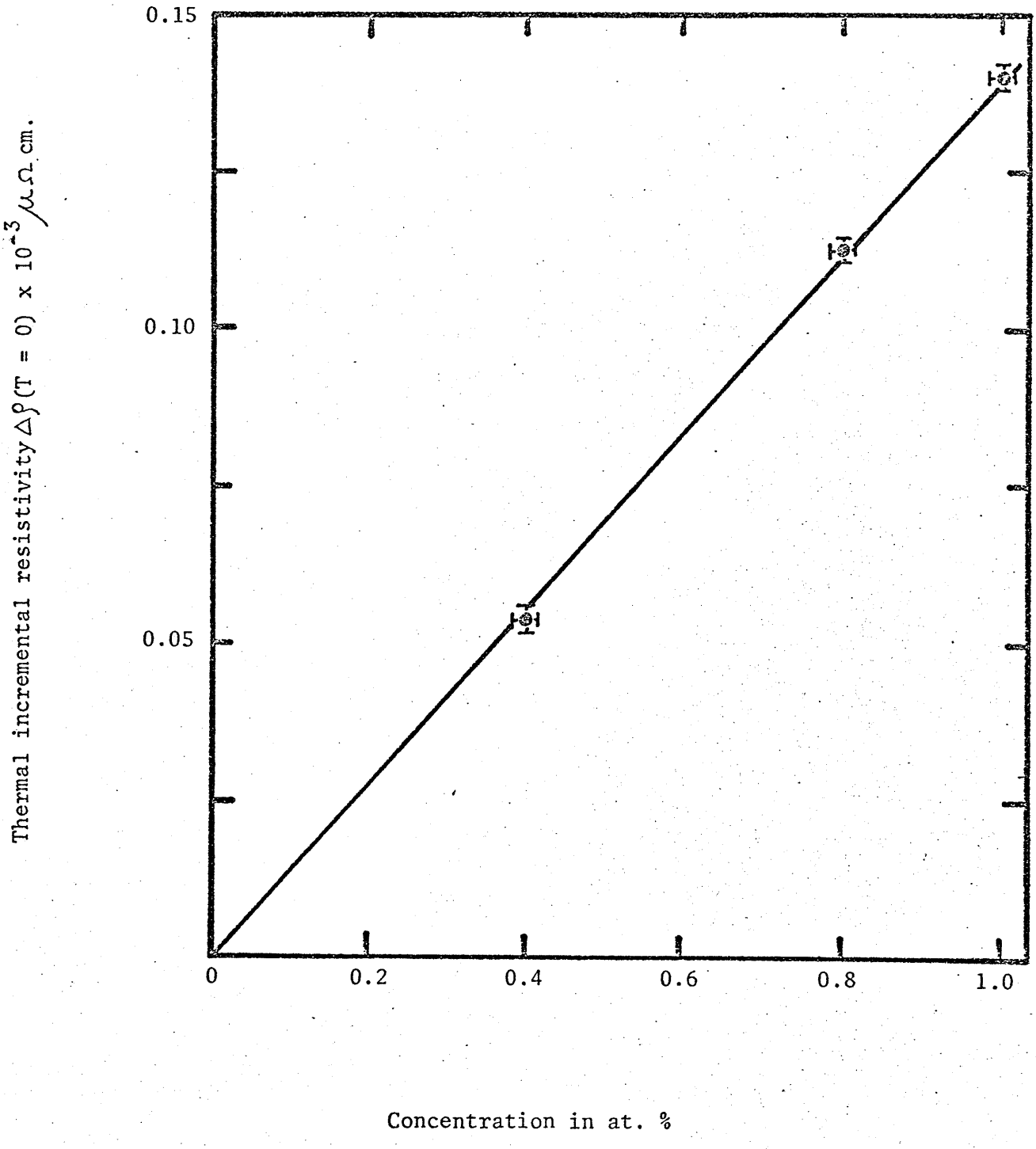
0.15
0.10
0.05
0
0.2
0.4
0.6
0.8
1.0
Thermal incremental resistivity $\Delta\rho(T = 0) \times 10^{-3}$ $\mu\Omega$ cm.
Concentration in at. %

Figure 3.7

The thermal part, $\Delta(T)$, of the incremental resistivity of Ru - 1. at.% Fe. The error bar represents the net effect of a ± 1.% shape factor uncertainty for both this alloy and the pure Ru sample.

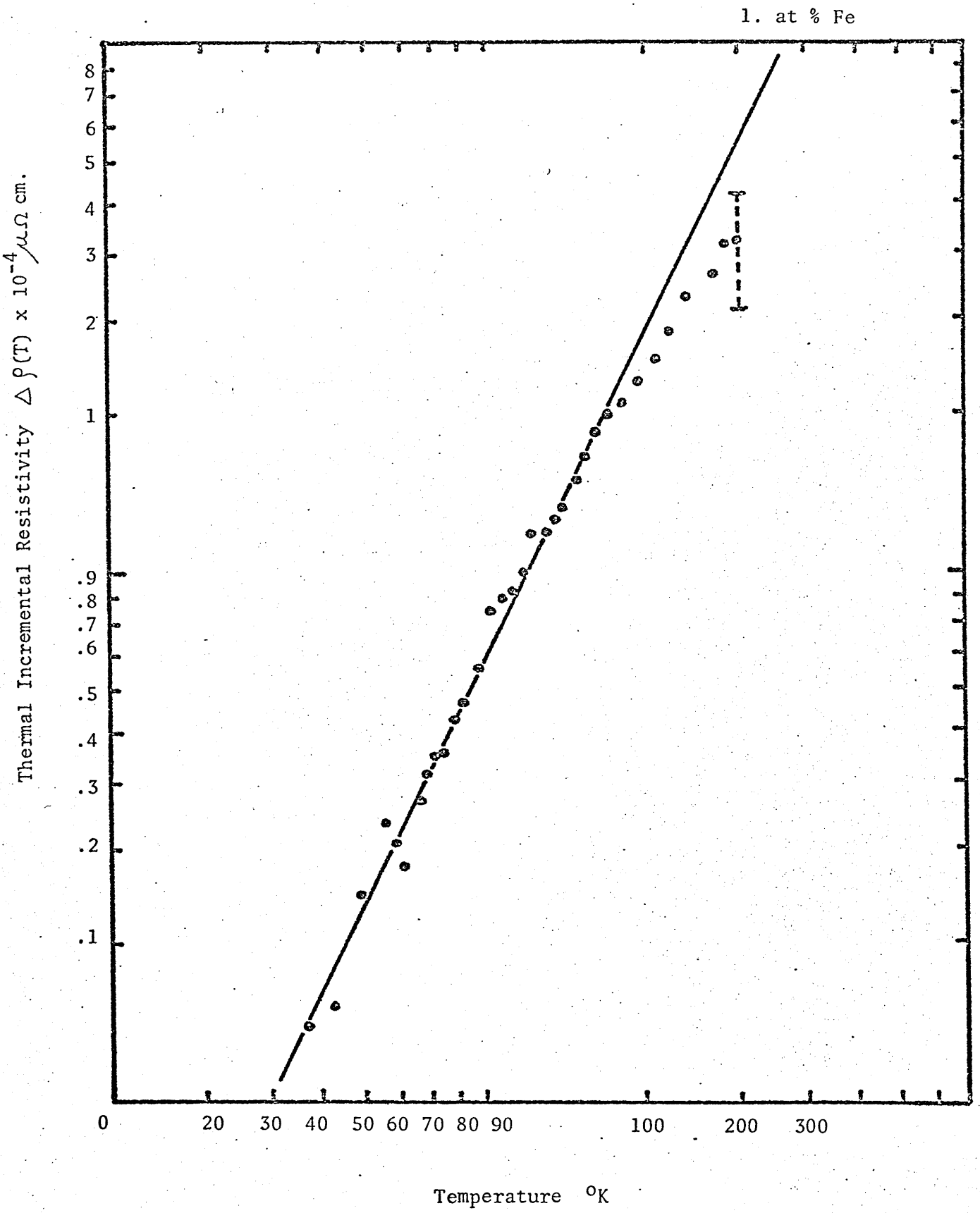
1. at % Fe
Thermal Incremental Resistivity Δρ(T) x 10^{-4} μΩ cm.
8
7
6
5
4
3
2
1
.9
.8
.7
.6
.5
.4
.3
.2
.1
0
20
30
40
50
60
70
80
90
100
200
300
Temperature °K

Figure 3.8

The thermal part, $\Delta(T)$, of the incremental resistivity of Ru - 0.8 at.% Fe. The error bar represents the net effect of a ±1.% shape factor uncertainty for both this alloy and the pure Ru sample.

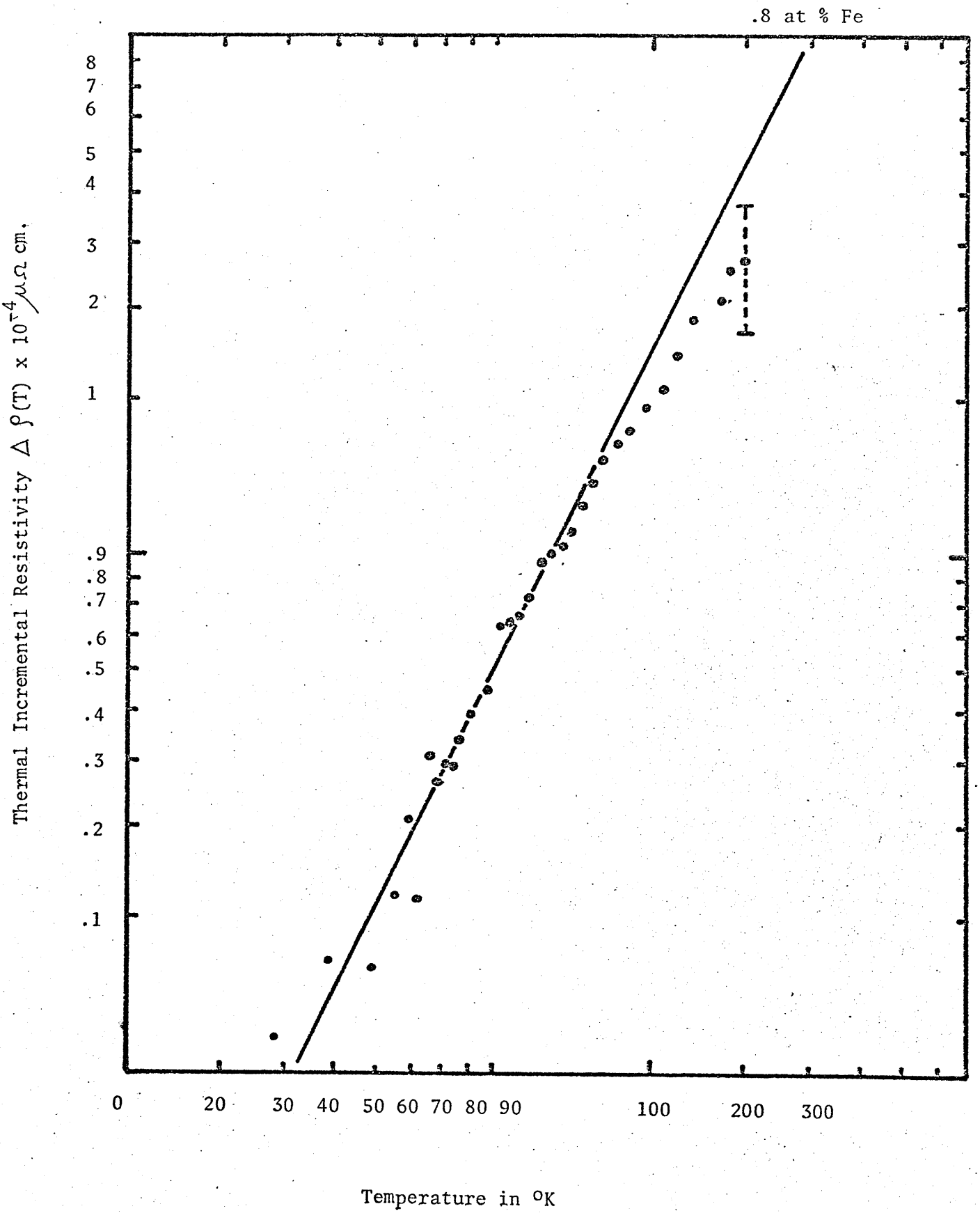
.8 at % Fe
Thermal Incremental Resistivity Δ ρ(T) x 10^{-4} μΩ cm.
8
7
6
5
4
3
2
1
.9
.8
.7
.6
.5
.4
.3
.2
.1
0
20
30
40
50
60
70
80
90
100
200
300
Temperature in °K

temperature relations.

$$\Delta(T) \propto T^2 \text{ for } T < \tfrac{1}{4}T_{sf}$$

$$\propto T \text{ for } T > 3/5\ T_{sf} \qquad 3.5$$

The range of temperature we are interested in our experiment is from 1.45°K to room temperature, and thus it is clear that our data do not extend to sufficiently high temperature to verify the linear temperature dependence predicted for (T). Yet T_{sf} can still be inferred from the low temperature data shown in Figures (3.7) and (3.8). Taking 175°K as the temperature at which the T^2 behaviour ceases, the spin fluctuation temperature T_{sf} for Fe in Ru is found to be about 700°K from Equation (3.5).

Experimental data obtained for 0.4 at. % Fe alloy are not included here, because the error arising from the form factor uncertainty corresponding to a substantial fraction of $\Delta(T)$ at all measuring temperatures —— $\Delta(T = 297^{\circ}K)$, for example, is $0.13 \pm 0.1\ \mu\Omega$ cm. The data obtained from this alloy, can only be used to set an upper limit on its T^2 coefficient. Within experimental error, the T^2 coefficient for the 0.4, 0.8, and 1.0 at. %. Fe alloys are listed in Table (3.4) scale with the normal Fe concentration.

Andres et al[22] (1969) measured the superconducting transition temperature T_c for Ru Fe alloys containing 1.8, 3.1 and 4.3 at. % Fe, and the data are reproduced in Figure (3.9) in which the ratio T_c/T_{co} (T_{co} is the transition temperature for pure Ru sample[23]) is plotted against the norminal Fe impurity concentration. In examining this figure, we observed that T_c is in fact suppressed rapidly by the addition of Fe atoms.[24] Andres et al, (1969) discussed this effect in terms of the decrease in electron-phonon attraction. Kaiser[25] (1970), taking into account localized spin fluctuations, has recently formulated a description of this depression in

Figure 3.9

The ratio T_C/T_{CO} for Ru Fe alloys from Andres et al. (1969), plotted against the normal Fe concentration. The error bars represent a ±0.1 at.% uncertainty in the Fe concentration. The full curve is a fit to Kaiser's (1970) expression as explained in the text.

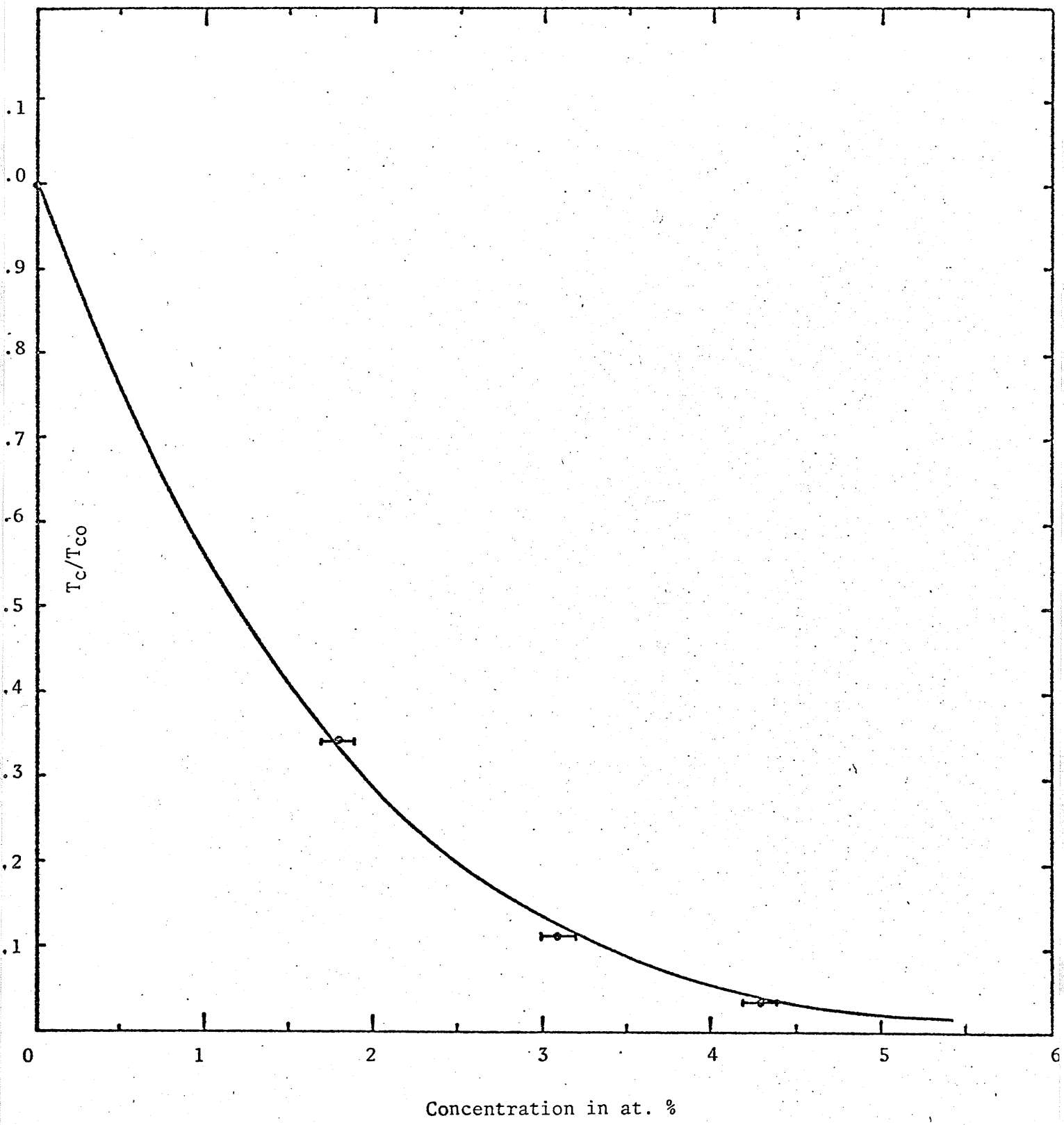
.1
.0
.9
.8
.7
.6
.5
.4
.3
.2
.1
T_c/T_{co}
0
1
2
3
4
5
6
Concentration in at. %

T_c (as a function of increasing impurity concentration) as a result of scattering of conduction electrons by the non-magnetic resonant impurity states, which at the same time, includes the effects of both an effective mass enhancement[26] and a strong intra impurity Coulomb repulsion[27]. The relation between T_c and the impurity concentration c is given by the following:[25]

$$\ln\left(\frac{T_c}{T_{co}}\right) = \frac{-(A + B)\,c}{g(1 - Bc)} \qquad 3.6$$

where $$A = \frac{N_i(E_F)}{N(E_F)} \qquad 3.7$$

and $$B = \frac{N_i^2(E_F)\ Ueff}{(2\ell + 1)gN(E_F)} \qquad 3.8$$

Here, $Ni(E_F)$ and $N(E_F)$ are the impurity and host density of states per spin direction at the Fermi level, respectively, g is the BCS coupling constant, while U_{eff} is the intra-impurity spin-up, and spin down coulomb repulsion $(2\ell + 1)$ accounts for orbital degeneracy. The values of A and B used for our fit to Andres data are listed in Table (3.5). The solid curve in Figure (3.9) represent the result of Kaiser's theory[25] —— a plot of Equation (3.6). The fact (see Figure (3.9)) that Andres results can be fitted to Kaiser's theory gives us supporting evidence for our assigning the origin of the temperature dependence in $\triangle(T)$ to localized spin fluctuations.

At sufficient low temperature, the expression for specific heat coefficient γ , for pure Ruthenium can be written as:-

Table 3.5

Summary of the parameters deduced from the depression of T_c in Ru Fe Alloys

A	B	$N_i(E_F)$ states/eV-atom-spin	U_{eff} (eV)	$N_i^*(E_F)$ states/eV-atom-spin	Δ (eV)	g
2.17	5.56	1.0	1.81	3.1	1.44	0.139

$$\gamma = \frac{2\pi^2}{3} N(E_F)\, k_B^2 (1 + \lambda) \qquad 3.9$$

where λ is the effective electron-phonon enhancement of the band density of states[28] and k_B is the Boltzmann's constant. With γ[29], found by Herninger, as 3.0 mJ/mol. deg^2 and λ = 0.38 from McMillan, $N(E_F)$ is found to be 0.46 states/eV-atom-spin.

From the values of A and B listed in Table (3.5) and Equation (3-7), the impurity density of state per spin direction at Fermi level $Ni(E_F)$ is found to be about 1.0 states/eV-atom-spin.

The BCS coupling constant g, appearing in Equation (3-8), can be obtained from the relation derived by Schrieffer[30] (1964):-

$$T_{co} = 1.14\, \theta_D \exp\left[-\frac{1}{g}\right] \qquad 3.10$$

With $T_{co}(Ru) = 0.48$[24] and Debye Temperature $\theta_D = 550^oK$ [29] then g = 0.139. Thus from Equation (3.8), U_{eff} has a value of 1.81eV.

While Kaiser's theory is based on the scattering of electrons by <u>non-magnetic</u> impurity states, it nevertheless explains the dependence of T_c/T_{co} on impurity concentration c in not only truely non-magnetic system like <u>Th</u> Ce[31], but also in localized spin fluctuation systems like <u>Al</u> Mn[32] and <u>Th</u> U[33]. In these latter system, $Ni(E_F)$ solved from Equation (3-7) are substantially smaller than those $Ni^*(E_F)$ estimated from the increase in γ on alloying, while Equation (3.8) leads to large values for U_{eff} (> 1. eV) compared with <u>Th</u> Ce. <u>Ru</u> Fe exhibits the characteristics of these latter l.s.f. systems, and the depression of T_c with impurity concentration c lies intermediate between <u>Th</u> Ce and <u>Al</u> Mn, with "large" U_{eff} and small $Ni(E_F) = (1/3)\, Ni^*(E_F)$. A comparison of the superconducting properties of <u>Ru</u> Fe

with both non-magnetic (Th Ce) and l.s.f. (Al Mn, Th U) systems thus provides supplimentary evidence supporting the present argument of l.s.f. at the Fe impurity sites in this system.

Within the framework of the Anderson[34] (1961) model, an estimation of the width Δ of the virtual bound state can be obtained from the following relation:-

$$N_i(E_F) = \frac{(2\ell + 1)}{\pi \Delta}\left[1 + \cot^2\left(\frac{\langle n \rangle \pi}{2(2\ell + 1)}\right)\right]^{-1} \qquad 3.11$$

Using the Hund's rule value of $\langle n \rangle = 6$, $\ell = 2$ and with $Ni(E_F)$ from Table (3.5), the value of Δ is found to be 1.44 eV.

Rivier and Machaughlin[35] have modified Equation (3.10) so as to include the effects of localized spin fluctuations. In the low impurity concentration limit, a comparison of the treatment of these latter authors with Equation (3.6) yields:-

$$T_{sf} \simeq \frac{A + B}{N(E_F)\ J^2 S(S+1)} \qquad 3.12$$

where J is the conduction electron-impurity coupling constant defined previously and S is the modulus of the fluctuating impurity "spin". With the values listed in Table (3.5), $|J| = 0.15$eV, and $S = 2$, (Hund's rule), the corresponding value of T_{sf} calculated from Equation (3-12) is about 700°K, which is in reasonable good agreement with the value we have deduced previously.

3.4 Summary

The resistivity of several dilute Ru Cr and Ru Fe alloys has been measured between 1.45°K and 300°K.

In Ru Cr system, the incremental resistivity is temperature independent at temperature below 30°K and from this we deduced that in the Static Hartree Fock context, Cr impurities in Ru are non-magnetic. At higher temperatures, deviations from Matthiessens rule have been observed and these can be fitted simply in terms of a "Two Current Model".

In the nearly isoelectronic Ru Fe system, a temperature dependent incremental resistivity $\Delta\rho(T)$ is observed. At temperature below 170°K, $\Delta\rho(T)$ increases as T^2, and less rapid at higher temperature. The origin of this tmeperature dependence is attributed to conduction electron scattering from ℓ.s.f. at the impurity sites, and the characteristic temperature T_{sf} in the Ru Fe system is about 700°K. Analysis of the existing experimental data on the depression of the superconducting transition temperature in Ru by Fe impurities using Kaiser's approach lends confirmatory evidence for such an assignment. Furthermore, the initial depression of T_c in this system allows a rough estimate of T_{sf} via the phenomenological expression of Rivier and Machaughlin, this latter estimate agrees reasonably well with that derived from our resistivity data.

Reference

1. G. Riblet, M. A. Jensen, Physica 55, 622, (1971).

2. K. Andres, E. Bucher, J. P. Marita, R. C. Sherweed, Phys. Rev. 178, 702-6 (1969).

3. A. J. Heeger, 'Solid State Phys." Vol. 23 Acad. Press. New York, 283, (1969).

4. A. D. Caplin, C. Rizzuto, Phys.RRev. Letters 21, 746, (1968).

5. F. C. C. Kao, Gwyn Williams, Phys. Rev. B, 7 267, (1973).

6. J. W. Loram, R. J. White, A. D. C. Grassie, Phys. Rev. B, Vol. 5 No. 9, 3659, (1972).

7. S. Shalski, M. P. Kawatra, J. A. Mydosh, J. I. Buduick, Phys. Rev. B, Vol. 2 No. 9, (1970).

8. Gwyn Williams, J. W. Loram, J. Phys. F. 1, 434, (1971).

9. M. D. Daybell, W. A. Steyert, Rev. Mod. Phys. 40 380, (1968).

10. J. W. Loram, T. E. Whall, P. J.Ford. Phys. Rev. B.2. 857, (1970).

11. R. M. Bozarth, P. A. Woeff, D. D. Davis, V. B. Compton, J. H. Wernick, Phys. Rev. 122, 1157, (1961).

12. W. B. Pearson 'Hand Book of Lattice Spacings and Structures of Metals', Pergamon Press, New York, (1958).

13. A. D. C. Grassie, G. A. Swallow, Gwyn Williams, J. W. Laram, Phys. Rev. B3 4154-60, (1970).

14. J. T. Schriempf, W. M. Macinnes, Phys. Letters 33A, 511-2, (1970).

15. G. K. White, S. B. Woods. Phil. Trans. Roy. Soc. A251, 273-302, (1959).

16. M. J. Rice, Phys. Rev. Letters 20, 1439-41, (1968).

17. J. S. Dugdale, Z. S. Basinski, Phys. Rev. 157 552-60, (1967).

18. J. Bass, Adv. in Phys. 21 431-604, (1972).

19. F. C. C. Kao, M. E. Colp. Gwyn Williams, Phys. Rev. B to be published, (1973).

20. A. B. Kaiser, S. Doniach, Int. J. Mag. 1, 11-22, (1970).

21. N. Rivier, V. Zlatic, J. Phys. F.2, L87-91, L99-104, (1972).

22. K. Andres, E. Bucher, J. P. Maita, R. C. Sherwood, Phys. Rev. 178, 702-6, (1969).

23. T. F. Smith Superconductivity in d- and f-band Metals. (New York: American Institute of Physics) pp. 293-320.

24. G. Riblet Phys. Rev. B. 3, No. 1, 91, (1971).

25. A. B. Kaiser, J. Phys. C.3 410-22, (1970).

26. M. J. Zuckermann, Phys. Rev. 140, A899-905, (1965).

27. C. F. Ratto, A. Blandin, Phys. Rev. 156, 513-21, (1967).

28. W. L. Mac Millan, Phys. Rev. 167, 330-44, (1968).

29. F. Heininger, E. Bucher, J. Muller, Phys. Kond. Materie 5, 243-9, (1966).

30. J. R. Schrieffer, Theory of Superconductivity (New York: Benjamin) pp. 169ff. (1964).

31. J. G. Huber, M. B. Maple, J. Low Temp. Phys. 3 537-44, (1970).

32. J. G. Huber, M. B. Maple, Solid State Commun. B. 1987-9, (1970).

33. M. B. Maple, J. G. Huber, B. R. Coles, A. C. Lawson, J. Low Temp. Phys. 3, 137-45, (1970).

34. P. W. Anderson, Phys. Rev. 124. 41-53, (1961).

35. N. Rivier, D. E. MacLaughlin, J. Phys. F. 1, L48-52 (1971).